**Siloxane Modified Polyurea and Polyurethane urea Segmented Copolymers**

by

Regina H. Kim

Thesis submitted to the Faculty of the

Virginia Polytechnic Institute and State University

in partial fulfillment of the requirements for the degree of

Master of Science

in

Materials Engineering

APPROVED:

| | |
|---|---|
| J. E. McGrath, Chairman | C. W. Spencer |
| G. L. Wilkes | J. P. Wightman |

August, 1989

Blacksburg, Virginia

**Siloxane Modified Polyurea and Polyurethane urea Segmented Copolymers**

by

Regina H. Kim

J.    E. McGrath, Chairman

Materials Engineering

(ABSTRACT)

High molecular weight polyether urea copolymers were synthesized using perfectly difunctional aromatic amine terminated polypropylene oxide (PPO) (2800 <Mn>) prepared via aluminum porphorin initiated coordination polymerization. The resulting segmented copolymer showed much higher tensile strength and better thermal stability than polyureas based on commercial PPO which contains some terminal unsaturation. This was attributed to the achievement of both higher molecular weight and to more extensive microphase separation between the segments. In addition, the surface structure of segmented polyether urea and polyurethane urea copolymers were modified in two ways: siloxane urea segmented copolymers were synthesized and physically blended into the system, and siloxane oligomers of controlled molecular weight and composition were incorporated into the copolymer backbone as a part of the soft segment. X-ray photoelectron spectroscopy (XPS) was used to obtain surface compositional information, while differential scanning calorimetry (DSC) and stress-strain analysis were used to characterize the bulk properties. In general, the surface enrichment of siloxane was observed in both solvent cast blends and siloxane incorporated systems. The surface siloxane concentration showed a small increase with siloxane segment length, content, and surface sensitive angle. Surface segregation of these systems was suppressed to a certain extent due to phase mixing within the copolymer bulk and by the anchoring of both ends of the siloxane segment with urea components. The bulk properties of these copolymer systems were not affected greatly when small amounts of siloxane ureas were added or when small amounts of siloxane blocks were incorporated.

# Acknowledgements

The author would like to express her gratitude to Dr. J. E. McGrath for his support and patience throughout this research effort.

The author would also like to extend her thanks to Dr. J. S. Riffle, Dr. Y. Yoo, C. A. Arnold and T. H. Yoon for their helpful suggestions.

Finally, she would like to express special thanks to her parents,                              , and

for their moral support.

# Table of Contents

# List of Illustrations

# List of Tables

# Chapter I. INTRODUCTION

The practice of adding surface active agents to modify polymer surfaces without markedly changing the bulk properties is not new. For example, addition of a low concentration of long chain fatty amides has long been used to reduce the friction coefficient of polyethylene films (1). Similarly, it has been observed that small amounts of fluorocarbon additives reduce the surface tension and coefficient of friction for a number of polymers such as polymethyl methacrylate, polyvinyl chloride, and polyvinylidene chloride copolymers (2).

Recently, it has become increasingly evident that block copolymers can also be utilized as surface active additives for polymer systems (3,4). When block copolymers containing low surface energy component is blended with a homo polymer possessing similar chemical structure as that of the high energy component, the lower energy block preferentially migrates to the polymer-air surface. This phenomena of surface enrichment by low energy component has been observed for many systems, especially when polysiloxane was used as one of the constituents.

In polystyrene-polysiloxane diblock copolymers studied, the surface layer was shown to consist of essentially polysiloxane component (5). Similar results were obtained from studies of polyurethane-polysiloxane systems (6). The surface composition of polycarbonate-polysiloxane copolymers investigated (7) also indicate siloxane domination at the surface.

When blended with polycarbonate homo polymer, siloxane was observed on the surface even at low concentrations of the copolymer. These results indicate that siloxane containing block copolymers have a high potential for commercial application as surface modifiers. Properties such as surface tension, wettability, friction, adhesion, and lubricity can be greatly effected by addition of such block copolymers.

The present research deals with the possible utilization of siloxane-urea segmented copolymers as surface additives for improving the lubricity of polyurethane/urea copolymers. The main aspects of the work will attempt to answer questions such as: Will the siloxane component migrate to the polymer-air surface in such blend systems? Would the surface behavior be different if the siloxane component was incorporated into the polyurethane/urea backbone rather than being physically added as a segmented copolymer? Would these systems be compatible in the sense that the surface properties are enhanced without detracting from the bulk properties greatly. The potential application of such blends is to obtain auto-withdrawing polyurethane/urea materials which could then be employed for both casting and reaction injection molding (RIM) processes.

Another aspect of the research is concerned with improving the mechanical properties of polypropylene oxide based segmented urea systems. The poor mechanical properties exhibited by these materials can be attributed in part to the poor functionality of the polypropylene oxide oligomers used which often contain monofunctional species and result in low molecular weight materials. The propylene oxide synthesized via living coordination polymerization in this laboratory (8) is highly difunctional and should improve the mechanical properties of segmented polyurea systems.

Therefore, the objectives of this research were to:

- to study the compatibility and surface properties of blends of polsiloxane-urea and polypropylene oxide-urea segmented copolymers.

- to investigate the surface and physical properties of polypropylene oxide-urea segmented copolymers when the siloxane segment is incorporated into the polymer backbone.

- to compare properties between polyureas based on commercial polypropylene oxide and well defined materials synthesized in this laboratory.

# Chapter II. LITERATURE REVIEW

## 2 - 1. Polyorganosiloxanes

### 2 - 1 - 1. Structure-Property Relationships

Polyorganosiloxanes are one of the most widely used class of semi-organic polymers due to its unique properties which allow applications in such industries as electrical, automotive, paint, textile, consumer products, cosmetic and medicine (8). The variety of useful and interesting properties exhibited by these materials stem from the characteristics of Si-O bonds, which are joined together in the polymer backbone with two organic substituents attached to the silicon atoms. The substituents can be alkyl, haloalkyl, and vinyl or phenyl groups depending on the specific properties desired.

The large Si-O-Si bond angle (144°) and C-Si-C bond angle (111°) allow ease of rotation about the Si-O and Si-C axis leading to high degree of flexibility and large intermolecular distances between siloxane chains (9). Consequently, weak intermolecular attraction between polymer chains result in low glass transition temperatures, Tg. The most common silicones,

polydimethylsiloxanes which have two methyl substituents, exhibit Tg of -123 °C, considered lowest among elastomers.

The high energy and polar nature of the Si-O bond are responsible for the thermal stability of siloxanes. They are resistent to oxidaton at temperatures up to 200 °C for long periods of time. However, when heated to 350 to 400 °C in inert atmosphere or in vacuum, polydimethylsiloxanes undergo depolymerization reaction, yielding lower cyclic siloxanes (10). But at 200 °C or higher, in the presence of air, cross-linking occurs rather than random scission. The high energy of Si-O bond (106 kcal), which is 30 kcal higher than C-C covalent bond, derives its strength from the unique nature of bonding between silicon and oxygen (11). Aside from the $\sigma$ type bonds between hybridized $s$ and $p$ electrons of the silicon atom with the $p$ electrons of the oxygen, additional $\pi$ type bonds exist from the combination of oxygen un-shared $p$ electrons and the silicon unfilled $3d$ orbitals. Thus, a partial double bond character is imparted, shortening the Si-O bond length (1.64 A°). This effect is further enhanced by the ionic character of the Si-O bond (approximately 50% ionic) arising from the electropositive nature of silicon atom.

Based on the electron diffraction and X-ray diffraction techniques, polysiloxane chain assums a helical configuration resulting from the tendency of the weak Si-O dipole to orient itself opposite another Si-O group in order to obtain intramolecular dipole stabilization (11). The helical structure consists of siloxane bonds which form the polymer backbone oriented towards the screw axis with the organic substituents protruding outwards to form a non-polar sheath around the polymer chain. Since the polar Si-O backbone is completely shielded by the hydrophobic organic substituents, low intermolecular forces exist between polymer chains. This leads to physical properties such as the hydrophobicity, high compressiblity, and low surface tension. The surface tension of linear polydimethylsiloxanes ranges from 15 to 22 dyn/cm and increases with increasing siloxane molecular weight (12). In addition, polysiloxanes also exhibit high gas permeability due to high free volume within its loosely packed structure, good UV and ozone resistance, good insulation properties, and good biocompatibility.

As mentioned earlier, the properties of polyorganosiloxanes can be affected by the substituent groups on the silicon (13). For example, the longer alkyl groups than methyl groups increase the lubricity and compatibility with organic compounds. The trifluoropropyl groups generally improve chemical and solvent resistance, while the phenyl substituents improve miscibility with the polar organic compounds.

## 2 - 1 - 2. Synthesis

A variety of routes are available for the synthesis of polysiloxanes which include (12): hydrolytic reactions of organohalosilanes or organoalkoxysilanes; redistribution type polymerization of cyclic monomers; anionic polymerization of the cyclic trimer, hexamethylcyclotrisiloxane; and a nonhydrolitic process by which organosilanes are reacted with alcohols or carboxylic acids, or organoalkoxysilanes with carboxylic acid. Only the first two methods are of commercial importance and both reactions involve a ring chain equilibrium distribution of products. In this laboratory, acid or base catalyzed equilibration technique was used to synthesize the functionally terminated polysiloxane oligomers. Therefore, the following discussion will focus on this process together with a brief description of synthesis of precursors for polysiloxanes.

In the equilibration process, the linear polysiloxanes are prepared via the anionic and cationic ring opening polymerization of cyclic siloxanes, which in turn are synthesized from hydrolysis of chlosilanes. Organochlorosilanes can be prepared from various techniques such as (12): a Grignard process; a redistribution process; a hydroxylation method; and a direct process. The latter method is most important in the commercial production of methylchlorosilanes and phenylchlorosilanes. The direct process involves the reaction of organic halides such as methyl chloride or chlorobenzene, with silicon or silicon alloys in a gas-solid reacton shown by:

$$2RX + Si \rightarrow R_2Si$$

The product of the reaction is a mixture of organohalosilanes, tetraalkylsilanes, organo-H-halosilanes, silicon tetrachloride, and small amounts of hydrocarbons formed by the recombination of organic radicals. The composition of the mixture can be affected by reaction conditions such as catalyst used, temperature, diluent gases, etc. For dimethyldichlorosilane, the main precursor for synthesis of polydimethylsiloxane, methylchloride is reacted with silicon at 250 - 300 °C in the presence of copper catalyst. The product mixture consists of 85 -90% dimethyldichlorosilane. In the case of diphenyldichlorosilane, a precursor for preparation of octaphenylcyclotetrasiloxane, chlorobenzene is reacted with silicon at 550 °C with silver as the catalyst. Approximately 50% of the reaction product is diphenyldichlorosilane.

Despite its commercial attractiveness, the direct process is inefficient for synthesis of other organosilanes (trifluoromethyl dichlorosilane, cyanoalkylchlorosilane, or vinylsilanes) due to extensive degradation during the reaction (14). Hence, hydrosilation method is generally used for these monomers. This method involves the addition of a compound with Si-H bond to an olefin, in the presence of transition metal catalyst.

The cyclosiloxanes are the starting materials for the synthesis of linear polysiloxanes, and can be prepared by the hydrolysis of chlorosilanes. The hydrolysis of dimethyldichlorosilane, shown in figure 1, yields a mixture of cyclic siloxanes and linear polysiloxane diols whose ratio can be controlled by varying the reaction conditions (12). For example, a high proportion of cyclics up to 90% octamethyltetracyclosiloxane, $D_4$, can be obtained if the hydrolysis is carried out with water in the presence of an organic solvent which is either slightly miscible or immiscible with water. This behavior was interpreted by suggesting that reduction of chlorosilanes in the aqueous phase will enhance the tendency for intramolecular condensation rather than intermolecular condensation, leading to higher concentration of cyclic siloxanes. On the other hand, predominantly linear high molecular weight polysiloxanes are obtained if the hydrolysis is carried out with 50 - 85% sulfuric acid due to

$$
\begin{array}{c}
CH_3 \\
| \\
Cl-Si-Cl + H_2O \\
| \\
CH_3
\end{array}
\longrightarrow
\quad
\begin{bmatrix}
CH_3 \\
| \\
Si-O \\
| \\
CH_3
\end{bmatrix}_n
\qquad n=3,4,5,\ldots,11
$$

$$
+
$$

$$
HO\begin{bmatrix}
CH_3 \\
| \\
Si-O \\
| \\
CH_3
\end{bmatrix}_n
\begin{array}{c}
CH_3 \\
| \\
Si-OH \\
| \\
CH_3
\end{array}
$$
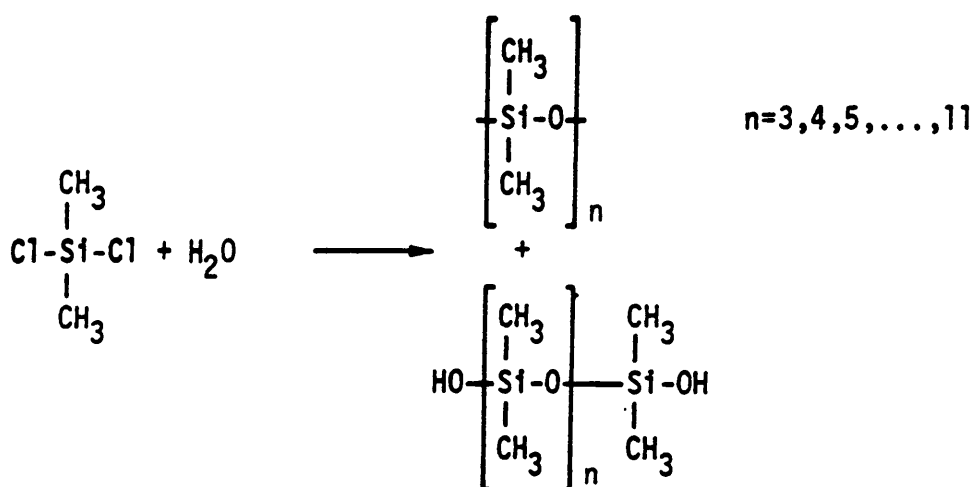
(1)    $Si-Cl + H_2O \rightleftharpoons SiOH + HCl$

(2)    $Si-OH + SiCl \rightleftharpoons Si-O-Si + HCl$

(3)    $Si-OH + HOSi \rightleftharpoons Si-O-Si + H_2O$

(4)    $2Si-Cl + H_2O \rightleftharpoons Si-O-Si + 2HCl$

Figure 1. Hydrolysis of dimethyldichlorosilane to yield $D_4$

acid catalyzed polymerization of cyclosiloxanes. The cyclic tetramer, $D_4''$, is also synthesized via similar hydrolysis process of diphenyldichlorosilane as shown in figure 2.

Linear polysiloxanes are most commonly synthesized by anionic or cationic ring opening polymerizations referred to as equilibration or redistribution reactions (15). The reactions mainly involve cleavage and reformation of Si-O bonds which at equilibrium result in product mixture of linear and cyclic siloxanes whose ratio depends on the reaction conditions and substituents on the silicon atom. A typical equilibration reaction with various other reactions which also occur are shown in figure 3. The nomenclature of "D" refers to a difunctional siloxane unit (usually dimethylsiloxy unit); "M" denotes a monofunctional siloxane unit; and "MM" is the linear dimer.

When both the linear disiloxane end-blocker and the cyclosiloxanes are present, the catalyst can attact the Si-O bonds of either species. If the cyclosiloxanes are attacked, chain propagation occurs resulting in higher molecular weight. If the end-blocker is attacked, it will result in chain transfer with the chain end, and further propagation of that chain is stopped. Thus, the molecular weight can be controlled by the ratio of the linear end-blocker to the cyclosiloxanes.

Due to the ionic character of Si-O bond which makes it susceptible to cleavage by acid or base, the reactions proceed via ionic mechanism under acid or base catalysts. The choice of catalyst depends upon the temperature of the equilibration as well as the type of funtional disiloxane used. For example, amine end groups would require a basic catalyst rather than an acidic catalyst which would react with the amine end group (15). For anionic polymerization, the active propagating species is a siloxanolate anion, while in the cationic case, the active species is thought to be the siliconium ion. Bases such as hydroxides, alcholates, phenolates and siloxanolates of the alkali metals, quaternary ammonium and phosphonium bases and the corresponding siloxanolates and fluorides, and organoalkali metal compounds are all known to catalyze the polymerization of cyclosiloxanes (16).

Catalysts based on quaternary ammonium and phosphonium hydroxides, silanolates and siloxanolates are called transient catalysts since they decompose above certain temper-
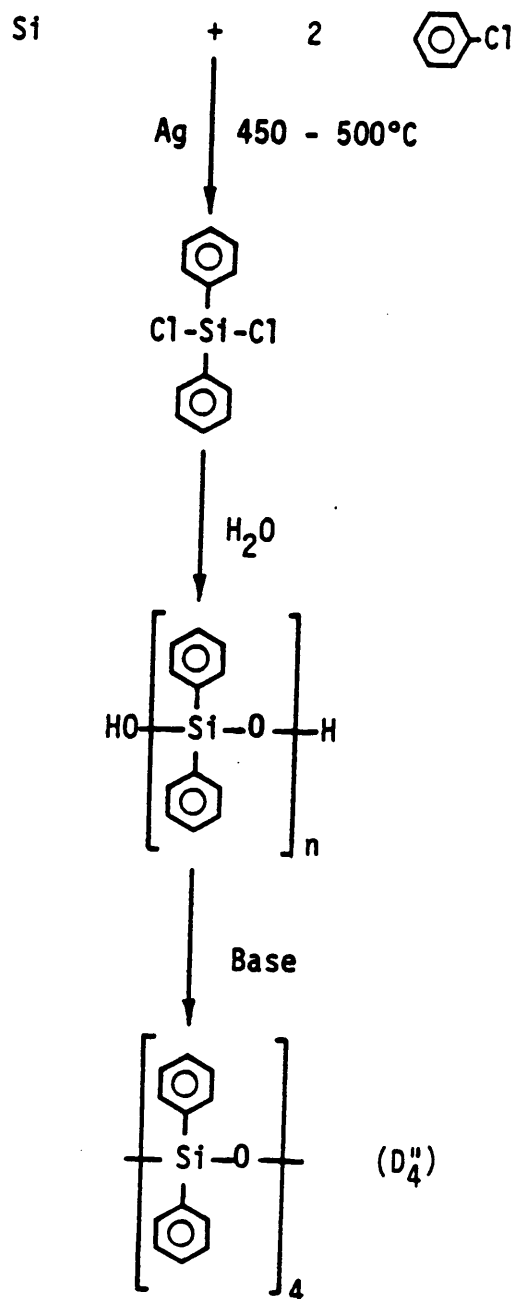
Figure 2. Hydrolysis of dimethyldichlorosilane to yield $D_4''$

$$\underset{\underset{CH_3}{|}}{\overset{\overset{CH_3}{|}}{R-Si}}-O-\underset{\underset{CH_3}{|}}{\overset{\overset{CH_3}{|}}{Si}}-R \quad + \quad \left[ \underset{\underset{CH_3}{|}}{\overset{\overset{CH_3}{|}}{Si}}-O \right]_4$$

$$\Delta \quad \Big| \quad \text{Catalyst}$$

$$R\left[ \underset{\underset{CH_3}{|}}{\overset{\overset{CH_3}{|}}{Si}}-O \right]_N \underset{\underset{CH_3}{|}}{\overset{\overset{CH_3}{|}}{Si}}-R$$

$$- D_x - \quad + \quad D_4 \quad \longrightarrow \quad - D_{(x+4)} -$$

$$- D_x - \quad + \quad MM \quad \longrightarrow \quad MD_x M$$

$$MD_x M \quad + \quad MM \quad \longrightarrow \quad MD_{(x-y)}M + MD_y M$$

$$MD_x M \quad + \quad MD_y M \quad \longrightarrow \quad MD_{(x+z)}M + MD_{(y-z)}M$$
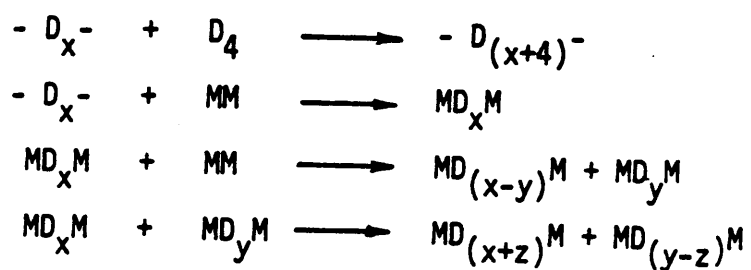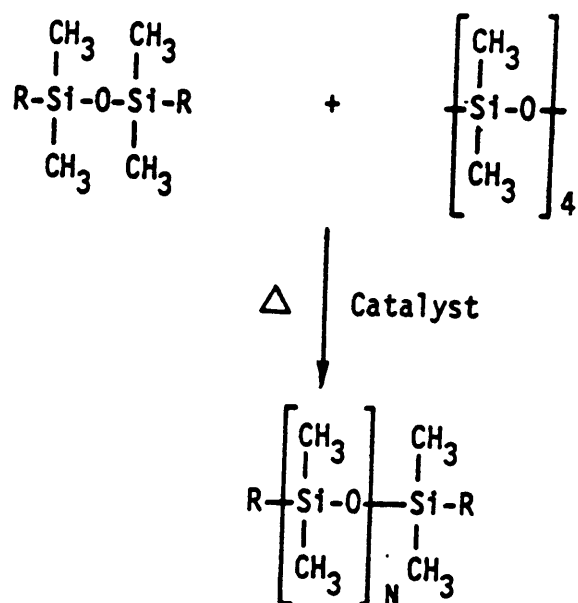
Figure 3. Equilibration reaction

atures to produce compounds which are not catalytically active toward siloxanes. For example, the tetramethylammonium siloxanolate catalyst polymerizes $D_4$ at temperatures up to 120 °C and decomposes above this temperature to methoxy terminated siloxane and trimethylamine which can be easily stripped off the reaction product. The phosphonium bases also decomposes thermally above 150 °C to give inert phosphine oxides and hydrocarbons. Unlike transient catalysts, others like potassium siloxanolate catalysts must be neutralized or removed to give a thermally stable polymer and prevent depolymerization at high temperatures.

As depicted in figure 4, the base catalyzed polymerization of cyclosiloxane involves the attack of the siloxanolate anion on the electropositive silicon atom of the cyclic or linear siloxane species (17). The reaction proceeds according to first order kinetics with a square root dependence on the catalyst concentration, as a result of tendency for the active centers to form ion pairs. The reaction rate increases with electronegative substituents such as phenyl and vinyl groups on the silicon atom which enhance the electron withdrawing effects, thus, facillitating the nucleophilic attack. The rate is also increased by the presence of polar aprotic donor solvents like tetrahydrofuran, dimethylformamide and sulfoxide (15). This effect was accredited to the solvation of the cations which allow the anion to attack the silicon atom with more ease. However, the addition of solvents will increase the amount of cyclics present in the product due to more prevalent back-biting reactions since the siloxanolate anion is less likely to encounter a cyclic in the dilute medium. Other studies have shown that the amount of cyclics present at equilibrium increases as the electronegativity, bulkiness or the polarity of the substituents increase (18).

The order of base catalyzed reactivity, where both the cyclosiloxane and the linear siloxanes are present, was determined to be (16):

$$D_3 > D_4 > MD_2M > MDM > MM$$

## Initiation

$$HO^{\ominus} \quad X^{\oplus} \quad + \quad -\overset{|}{\underset{|}{Si}}_1 - O - \overset{|}{\underset{|}{Si}}_2 \quad \longrightarrow \quad HO - \overset{|}{\underset{|}{Si}}_1 - \quad + \quad X^{\oplus} \quad O^{\ominus} - \overset{|}{\underset{|}{Si}}_2 -$$

$$-\overset{|}{\underset{|}{Si}}_2 - O^{\ominus} \quad X^{\oplus} \quad \rightleftharpoons \quad -\overset{|}{\underset{|}{Si}}_2 - O^{\ominus} \quad + \quad X^{\oplus}$$

## Propagation

$$-\overset{|}{\underset{|}{Si}}_2 - O^{\ominus} \quad + \quad -\overset{|}{\underset{|}{Si}}_3 - O - \overset{|}{\underset{|}{Si}}_4 \quad \longrightarrow \quad -\overset{|}{\underset{|}{Si}}_2 - O - \overset{|}{\underset{|}{Si}}_3 - \quad + \quad -\overset{|}{\underset{|}{Si}}_4 - O^{\ominus}$$
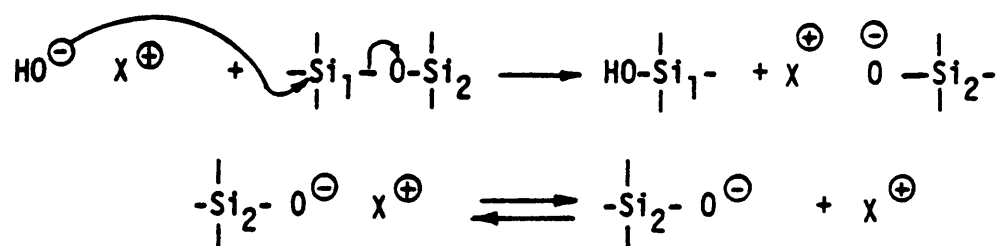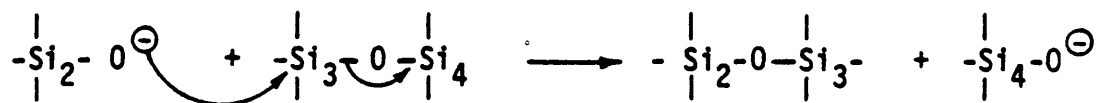
Figure 4. Base catalyzed polymerization mechanism

Since the anion attacks the cyclosiloxane before attacking the disiloxane MM, the reaction mixture proceeds through a viscosity maximum followed by a viscosity decrease as the disiloxane equilibrates into the chain.

However, this viscosity maximum was not observed when a sulfuric acid catalyst was employed. Also, the activity of the siloxanes towards equilibration was found to be reverse the order of a base catalyzed equilibration (17):

$$D_3 < MM < MDM < MD_2M < D_4$$

Since the acid catalyst atacks the more basic disiloxane MM prior to the cyclosiloxane, the reaction does not proceed through a viscosity maximum.

The acid catalyzed polymerization of cyclosiloxanes have been less studied than the anionic case. The most frequently employed acid catalysts include sulfuric acid and its de-rivatives, generally used with end blockers containing functional end groups such as alkyl linked carboxylic acid or cyanoethyl end groups (18). The suggested mechanism of acid catalyzed polymerization is illustrated in figure 5 (15). The protonation of oxygen atom in the cyclosiloxane occurs first, followed by the cleavage of the Si-O bond to give a silanol end group and possibly a siliconium cation which has been postulated as the active center of the propagating species. The rate of reaction increases with electron donating groups present on the silicon atom and decreases with electron withdrawing substituents.

The anionic copolymerization of $D_4$ and $D_4''$ has also been studied to a limited extent because of the difficulty arising from the crystallinity of cyclic tetramer $D_4''$. The equilibration proceeds via base catalysis since the resonance and steric effects of the phenyl groups render the silicon atom to be more electropositive. Consequently, the Si-O bond becomes less sus-ceptible to acid attack. The kinetic studies (19) with KOH and NaOH catalysts have shown that $D_4$ polymerizes only after the dissapearance of $D_4''$. The presence of the weaker diphenyl siloxane anion was thought to decrease the rate of $D_4$ polymerization. In a different kinetic study (20), $D_4$ was observed to polymerize early rather than after $D_4''$, with the copolymer

## Initiation
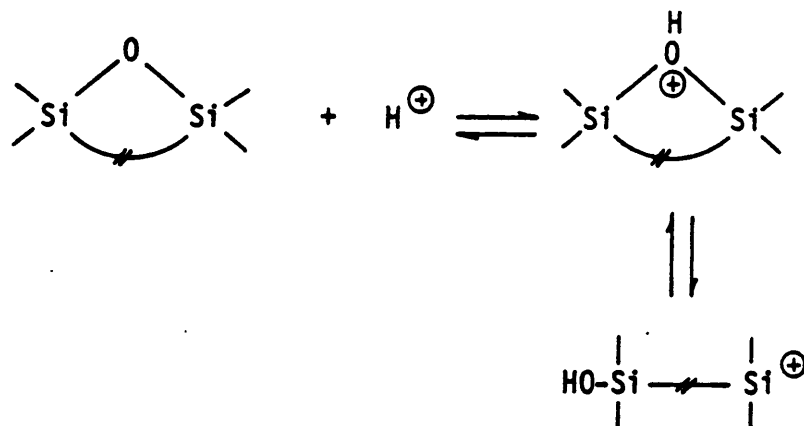


## Propagation
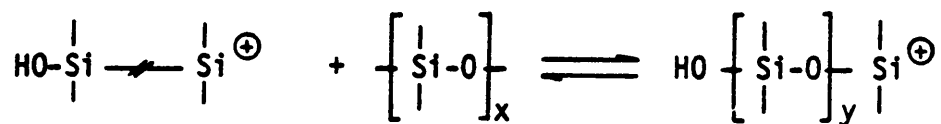


Figure 5. Acid catalyzed polymerization mechanism

composition containing larger proportion of diphenyl siloxane units. The rate of the copolymer formation was found to decrease with increasing $D_4$ concentration in the initial reaction mixture. Further investigations must be carried out before this system is well understood.

## 2 - 1 - 3. Block Copolymers of Siloxane

Siloxane containing block or segmented copolymers have been synthesized since the early 1950's, with the purpose of improving properties such as broader range of service temperature, surface characteristics, thermal and oxidative stability, impact modifier, and melt processiblity to mention a few. Today, the blocks which have been copolymerized with polysiloxanes include: polyolefin, polyether, polycarbonate, polysulfone, polyurethane and urea, and polyimide (21). In this section, the synthesis and properties of some of the commercially attractive and widely studied copolymers will be summarized briefly.

Diblock copolymers containing polystyrene and polydimethylsiloxane have been prepared by anionic polymerization. The polystyryl anion was generated first, followed by initiation and polymerization of the cyclic organosiloxane tetramer or trimer (22). The two phase morphology of the resulting polymer has been observed to vary with the solvent employed in casting the films (23). The anionic copolymerization method has not been very successful due to siloxane homopolymer contamination from the redistribution of siloxane cyclics, especially for the case of the tetramer (24). The reaction of polystyryllithium with cyclotrisiloxanes have led to better defined structures of styrene-siloxane block copolymer, since the lithium silanolates do not cause siloxane equilibration.

Siloxane-styrene-siloxane triblock copolymers have also been synthesized via step-growth or condensation copolymerization of preformed difunctional siloxane and styrene oligomers. The studies of reactions of allyl terminated polystyrene oligomers with silyl terminated polysiloxane oligomers; and disilanol terminated polystyrenes with dichloro terminated polysiloxane have been reported (21, 25). For the styrene-siloxane-styrene triblocks,

different synthetic routes were used. Either the dichloro terminated polysiloxane were capped with polystyryl anions (21), or polystyrene-polysiloxane anions were coupled with chlorinated coupling agents (22).

Styrene-siloxane multi-block copolymers were prepared by generating a polystyryl dianion to initiate the polymerization of hexamethylcyclotrisiloxane (28). This was followed by coupling the disilanolate terminated siloxane-styrene-siloxane segmented dianions together with silane coupling agents. When blended with polystyrene homopolymers, these styrene-siloxane copolymers were found to improve the lubricity and reduce the surface tension of the polystyrene (29).

Polysiloxane-polyether copolymers can have Si-O-C or Si-C linkages between the two types of polymer blocks. Copolymers with Si-O-C linkages are usually synthesized by reacting dihydroxy terminated polyether oligomers with siloxanes containing functional end groups of acetoxy, alkoxy, silyl chloride or silyl hydride (21). The Si-C bridge can be prepared by the addition of Si-H bonds to polyethers containing alkenyl groups, or by the reaction of organo functional polysiloxanes with polyether glycols (30). The latter type of linkages are considered more hydrolytically stable. Both hydrophobic siloxane and hydrophilic polyether blocks within the copolymer have led to many applications, especially as effective polyurethane foam stabilizers.

Well-defined multi-block copolymers of polydimethylsiloxane and polysulfone have been synthesized via silylamine-hydroxyl condensation reactions (31). The polysiloxane-polysulfone copolymers showed microphase separation even at low block molecular weights due to large solubility differences between the blocks (32). The incompatibility between the blocks have resulted in poor processibility (33). However, the copolymers improve impact property and stress crack resistance of polysulfone when blended with the polysulfone homopolymer (34).

Polysiloxane-polycarbonate block copolymers can be synthesized in several ways. One of the synthetic routes involves capping the dichloro terminated polysiloxane oligomers with an excess of bisphenol-A, followed by phosgenation (35). Another method involves the re-

action of hydroxy terminated siloxane oligomers, bisphenol-A, and phosgene in the presence of a tertiary amine (30). Well defined perfectly alternating block copolymers can be prepared by silylamine-hydroxyl condensation reaction of pre-prepared dihydroxyl terminated polycarbonate and dimethylamine terminated polysiloxane oligomers (36). The copolymers exhibit two phase morphology with both the morphology and mechanical properties varying with the copolymer composition and block molecular weights (37). These materials retain the low temperature properties of the siloxane block, yet are strengthened by the presence of polycarbonate blocks. In blends with polycarbonate homopolymer, friction and wettability resistance are improved (38).

Segmented copolymers of polysiloxane-polyurethane and polysiloxane-polyurea have been synthesized from the condensation reaction of 4, 4'-diphenylmethane diisocyanate (MDI) or toluene diisocyanate (TDI) with hydroxyl terminated and amine terminated polysiloxane oligomers respectively (39, 40). Good elastomeric properties were observed with potential uses as adhesives, coatings and surface modifiers. Synthesis of imide-siloxane segmented copolymers have been also reported, where a poly(amic acid- siloxane) precursor was first prepared, followed by either thermal or solution imidization (41). The incorporation of siloxane segments were observed to improve the flow properties and modify the surface characteristics.

## 2 - 2. Segmented Polyurethanes

Segmented polyurethanes and polyureas are multi-block copolymers consisting of alternating sequence of hard and soft segment units. Due to incompatibility between the two types of structural units, the polymer undergoes a microphase separation resulting in hard segment rich domains, soft segment rich matrix and their interphase. The hard segment domains, their Tg or Tm above the usual service temperature, act as physical crosslinks for the soft segments. This two phase morphology accounts for the desirable thermoplastic and

## Table 1. Examples of conventional polyol soft segments

### POLYESTER TYPE

Poly(tetramethylene adipate) glycol

$$\{\overset{O}{\overset{\|}{C}}O(CH_2)_4-\overset{O}{\overset{\|}{C}}-O(CH_2)_4O\}_n$$
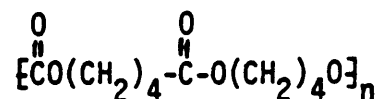
Poly(caprolactone) glycol

$$\{(CH_2)_5-\overset{O}{\overset{\|}{C}}-O\}_n$$
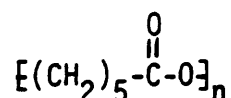
Po(hexamethylene carbonate) glycol

$$\{(CH_2)_6-O-\overset{O}{\overset{\|}{C}}-O-\}_n$$
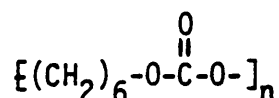
### POLYETHER TYPE

Poly(tetramethylene oxide) glycol

$$\{O-(CH_2)_4\}_n$$
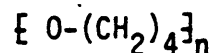
Poly(1,2-oxypropylene) glycol

$$\{O-\underset{\underset{CH_3}{|}}{CH}-CH_2\}_n$$
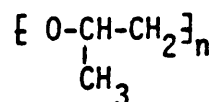
## Table 2. Examples of widely used diisocyanates

OCN—⬡—CH$_2$—⬡—NCO
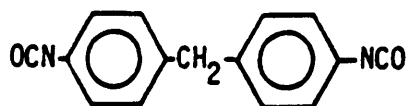
4,4'-Diphenylmethane Diisocyanate (MDI)
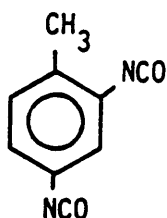
2,4-Toluene Diisocyanate (2,4,-TDI)   2,6-Toluene Diisocyanate(2,6-TDI)
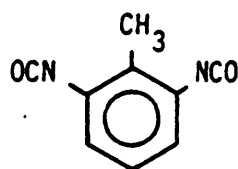
OCN- (CH$_2$)$_6$ -NCO
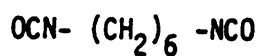
Hexamethylene Diisocyanate

OCN—⬡—CH$_2$—⬡—NCO
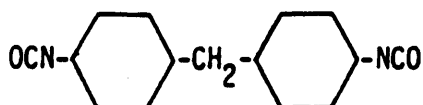
4,4'-Dicyclohexylmethane Diisocyanate (H-MDI)     p-Phenylene Diisocyanate
                                                  (p-PDI)
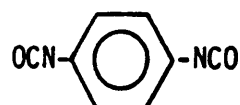
OCN—⬡—NCO

OCN—⬡—CH$_2$—⬡—NCO
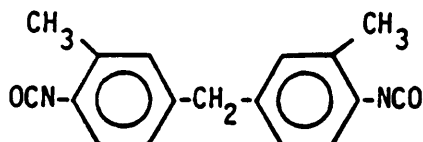
3,3'-Dimethyl-Diphenylmethane 4,4'-Diisocyanate

Table 3. Typical chain extenders

<u>DIOL CHAIN EXTENDERS</u>

| | |
|---|---|
| Ethylene Glycol | $HO-CH_2-CH_2-OH$ |
| 1,3-Propane Diol | $HO-CH_2-CH_2-CH_2-OH$ |
| 1,4-Butanediol | $HO-CH_2-CH_2-CH_2-CH_2-OH$ |
| 1,4-Pentanediol | $HO-(CH_2)_5-OH$ |
| 1,6-Hexanediol | $HO-(CH_2)_6-OH$ |
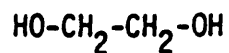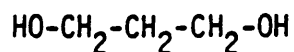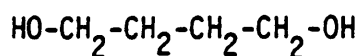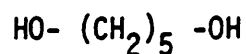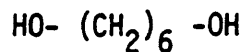
<u>DIAMINE CHAIN EXTENDERS</u>

3,3'-Dichloro-4,4'-Diaminodiphenylmethane (MOCA)
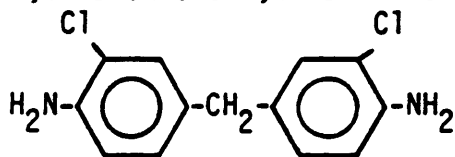


4,4'-Diaminodiphenylmethane
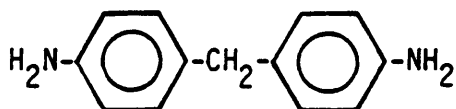


1,4-Diaminobenzene



Ethylenediamine

$H_2N-CH_2CH_2NH_2$
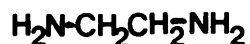
elastomeric properties in segmented polyurethanes leading to its commercial importance. This section will briefly review the synthesis, structure- property relationships, and morphology of segmented polyurethanes.

## 2 - 2 - 1. Synthesis

The segmented polyurethanes are synthesized by the step growth polymerization of three basic building blocks: the polyol, diisocyanate, and chain extender. The polyol which make up the soft segment is typically composed of hydroxyl terminated polyester or polyether with molecular weights ranging between 1000 - 3000 g/mol. The hard segment consists of a diisocyanate reacted with a diol or a diamine chain extender. Examples of commonly used components are shown in tables 1, 2, and 3.

The chemistry of urethane formation involves the isocyanate groups (-NCO) reacting with active hydrogen atoms of polyol and the chain extender (44). The isocyanate groups react with hydroxyl groups to form urethane linkages; with amines to form urea linkages; and with water to produce ureas and carbon dioxide as shown in figure 6. The latter reaction is of interest when forming foamed products. Other side reactions can also occur which result in branching and cross-linking. Allophanate groups are formed by the reaction of isocyanate with urethanes; biuret, from isocyanates and ureas; and trimers from the reaction of three isocyanates. To obtain linear high molecular weight products, reaction conditions of difunctional reactants, exact stoichiometry, and minimal side reactions are critical.

Two synthetic methods are used in preparing segmented polyurethanes (44): the one-step and the prepolymer process as illustrated in figures 7 and 8. In the one-step route, the entire polymer formation is carried out by simultaneously mixing together polyol, diisocyanate, and chain extender. Alternatively, in the prepolymer method, the final polymer is formed in two steps. Initially, excess diisocyanate and polyol are reacted to form isocyanate end capped polyol (prepolymer), followed by addition of chain extender in molar proportions

RNCO + R'OH $\longrightarrow$ RNHCOOR'   urethane

RNCO + R'NH$_2$ $\longrightarrow$ RNHCONHR'   urea

RNCO + R'COOH $\longrightarrow$ RNHCOR'   amide + $CO_2$

RNCO + H$_2$O $\longrightarrow$ [RNHCOOH]   carbamic acid

$\longrightarrow$ RNH$_2$ + CO$_2$ $\xrightarrow{\text{RNCO}}$ RNHCONHR   urea


-RNCO + -R'NCOR'- $\longrightarrow$ -R'NCOR'-
         |                    |
         H                    CONHR-

         amide                acylurea


                H
                |
-RNCO + -R'NCONR'- $\rightleftharpoons$ -R'NCONHR'-
         |                    |
         H                    CONHR-

         urea                 biuret


-RNCO + -R'NCOOR'- $\rightleftharpoons$ -R'NCOOR'-
         |                    |
         H                    CONHR-

         urethane             allophanate
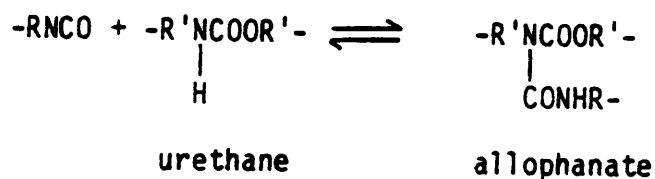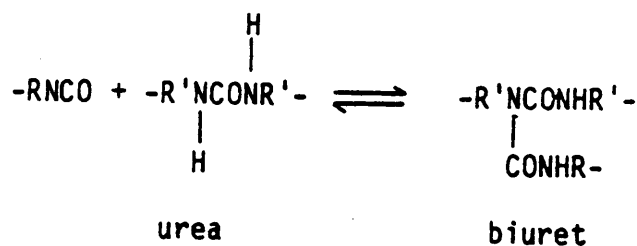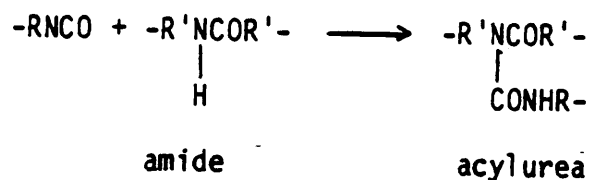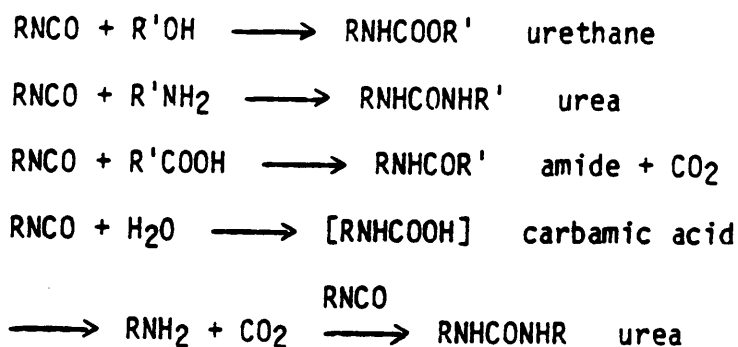

Figure 6. Reactions of isocyanates

equal to the free isocyanate groups available. The reaction of chain extender with both high and low molecular weight isocyanate groups is statistical, and the resulting structure is not perfectly alternating, with blocks themselves being quite polydisperse (21). The latter method offers better reaction control and result in narrower molecular weight distribution of the hard segment lengths.


## 2 - 2 - 2. Structure-Property Relationships


The wide range of physical properties and morphologies possible by changing the chemical components and composition has generated a great deal of interest in structure-property relationships, in order to tailor materials for specific applications.

The nature of soft segment generally controls the low temperature properties and the extensibility of the system. Therefore, factors such as soft segment glass transition temperature, crystallizability, molecular weight, and compatibility with hard segments are very important (45-47). Conventional polyols used are linear aliphatic polyesters or polyethers, where polyurethanes based on polyethers tend to show better hydrolysis resistance and poorer oxidative stability (48). However, polyester based polyurethanes display better physical and mechanical properties than polyether based materials due to higher degree of hydrogen bonding present (49). They also exhibit higher degree of phase mixing as a result of more polar nature of the ester group. This leads to poor hysteresis behavior as the hard domains which are disrupted under deformation is not recovered instantaneously upon the removal of stress (50).

Recently, polyurethanes incorporating soft segment polyols based on polyisobutylene (PIB), polybutadiene (PBD), and polydimethylsiloxane (PDMS) have also been introduced (51-53). Some advantageous properties of these materials include improved low temperature flexibility and higher oxidative stability. But, lower tensile properties relative to those of conventional polyether or polyester polyurethanes have been observed. This was attributed to

Diol chain extension

$$HO—A—OH \quad + \quad OCN—R_1—OCN \quad + \quad HO—R_2—OH$$

Linear polyester or      Diisocyanate      Low molecular weight
polyether diol                               diol

Structure repeating unit

$$\left[ \overset{O}{\overset{\|}{C}}—NH—R_1—NH—\overset{O}{\overset{\|}{C}}—O—A—O—\left( \overset{O}{\overset{\|}{C}}—NH—R_1—NH—\overset{O}{\overset{\|}{C}}—O—R_2—O \right)_x \right]_n$$

Isocyanate      Low molecular weight diol

Polyester or polyether | Urethane     Urethane

Flexible segment      Rigid segment
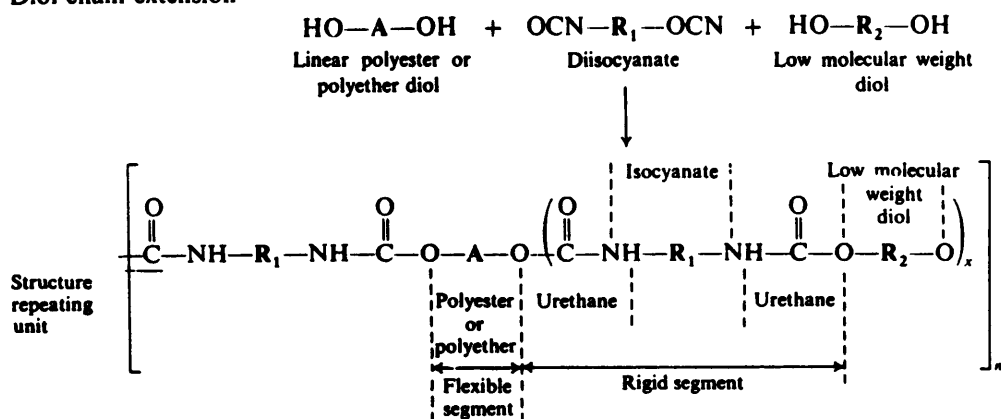
*or*

Diamine chain extension

$$HO—A—OH + OCN—R_1—NCO + H_2N—R_3—NH_2$$

Repeating unit

$$\left[ \overset{O}{\overset{\|}{C}}—NH—R_1—NH—\overset{O}{\overset{\|}{C}}—O—A—O—\left( \overset{O}{\overset{\|}{C}}—NH—R_1—NH—\overset{O}{\overset{\|}{C}}—NH—R_3—NH \right)_x \right]_n$$

Flexible segment      Urea

Rigid segment
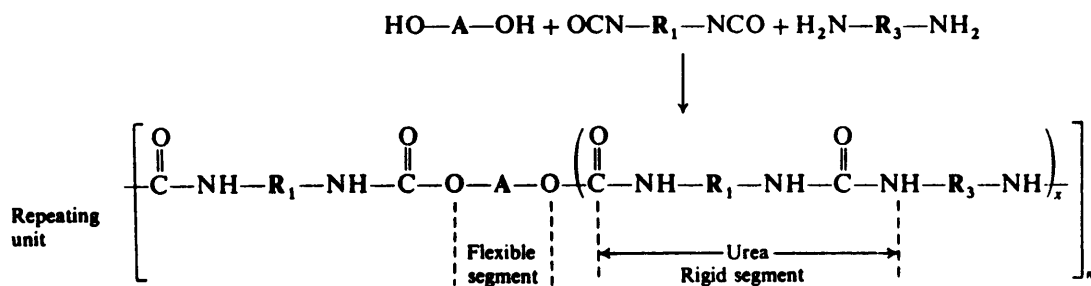
Figure 7. One step process (44)

HO—A—OH    +    NCO—R$_1$—NCO

Linear polymeric          Difunctional diisocyanate
glycol

$$NCO—R—NH\overset{O}{\overset{\|}{C}}—O—A—O—\overset{O}{\overset{\|}{C}}NH—R_1—NCO$$

Prepolymer

Chain extension: this is usually
by one of two routes

Route 1. Dihydric glycol
chain extension
$(n-1)$HO—R$_2$—OH

Route 2

Urethane        Urethane

$$\left[O—A—O—\overset{O}{\overset{\|}{C}}NH—R_1—NH—\overset{O}{\overset{\|}{C}}\left(O—R_2—O—\overset{O}{\overset{\|}{C}}—NH—R_1—NH—\overset{O}{\overset{\|}{C}}\right)_{n-1}\right]$$

Soft
segment

|← Hard segment →|

Route 2 uses a diamine
chain extender H$_2$N—R$_3$—NH$_2$

Urethane      Isocyanate        Diamine
              nucleus           segment
              Urea segment

$$\left[O—A—O—\overset{O}{\overset{\|}{C}}—NH—R_1—NH\left(\overset{O}{\overset{\|}{C}}—NH—R_3—NH—\overset{O}{\overset{\|}{C}}—NH—R_1—NH·—\overset{O}{\overset{\|}{C}}\right)_{n-1}\right]$$

Soft
segment

|← Hard segment →|

Figure 8. Prepolymer process (44)

lower soft segment Tg, a lack of soft segment crystallizability under strain, and an excessively high degree of phase separation which result in premature phase separation during polymerization leading to low molecular weight (54).

The effect of soft segment molecular weight on the properties of conventional polyurethanes have been investigated extensively (55, 56). In most cases, optimum properties were obtained when the soft segment molecular weights ranged between 2000 to 3000 g/mol. Decrease in the soft segment molecular weight resulted in lower degree of phase separation and loss of ability to undergo strain induced crystallization leading to poorer tensile properties.

The effects of soft segment length distribution on the mechanical properties have also been studied (21, 57). The results show that narrow soft segment distribution causes a slight increase in modulus, a moderate increase in tensile and elongation, and a large increase in extension set.

The hard segments are the product of reaction between diisocyanate with a diol or a diamine, and act as physical crosslinking sites reinforcing the soft segment matrix. Consequently, chemical structure of the hard segments play a decisive role in determining the mechanical performance of the segmented polyurethanes at higher temperatures. Structural linearity, symmetry, and aromaticity of the isocyanates yield higher modulus, tensile and tear strength materials, by providing rigidity and facilitating hard segment crystallization (57). Similar conclusions were reached from the study of various chain extenders used (58). Those having aromatic structures provided greater tensile strength than their aliphatic counterparts.

For both the aliphatic and aromatic extenders, structural symmetry and linearity promoted higher mechanical strength and elasticity, and lower damping characteristics. Generally, the use of a diamine chain extender instead of a diol, results in higher mechanical strength due to stronger hydrogen bonding interactions in urea linkages compared to urethane linkages. In the case of aliphatic diols, the length of the diol can also affect the physical properties (59). Those with even number of methylene carbons gave superior properties than those with odd numbers of methylene carbons. This was attributed to favorable

packing arrangements between two polymeric chains which favor highest intermolecular hydrogen bonding. Conversely, in the study of aliphatic diamines with varying chain length, the hard segments based on an odd number of methylene units were found to display higher tensile strength and elongation at break (44). It was suggested that random packing of chains led to lower modulus and higher elongation which subsequently affected the soft segment crystallization in this particular system.

The effects of hard segment size, distribution and content on mechanical properties of segmented polyurethanes show following trends (57, 60, 61). Increase in hard segment size and content is usually accompanied by an increase in modulus, tensile strength and extension set, and decrease in elongation at break. Similar effect is achieved by narrowing the hard segment distribution.


## 2 - 2 - 3. Morphology


Since Cooper and Tobolsky (62) first postulated a phase separated structure for segmented polyurethanes, a considerable effort has been devoted to the characterization of hard and soft segment microdomains. But the complexities of multi-block structure with variable block length as well as possible crystallinity of hard or soft segments and hydrogen bonding have proved to make the task most difficult.

The first direct evidence for the formation of a two phase structure was from the small angle x-ray scattering (SAXS) studies by Bonart and Clough et al (63, 64). A prominent scattering peak observed at low angle, corresponding to a long spacing of about 10 - 25 nm, was interpreted as being related to the interlamellar distance between microdomains. It was also observed that SAXS intensity changed in an orderly fashion as the composition of the material changed. This was attributed to the degree of aggregation of the hard segments or the degree of phase separation.

The majority of the early investigations have concentrated on the determination of this degree of microphase separation through the application of scattering techniques, or by analysis of the soft microdomain glass transition temperatures obtained from differential scanning calorimetry (DSC) and dynamic mechanical calorimetry (65). However, each of these methods suffer from limitations. SAXS invariant calculations clearly show that microphase separation is incomplete but cannot specify values for compositions of the individual domains (66). Although quantitative analysis of Tg behavior has been carried out, the complete description of microdomain mixing from DSC measurements has been hindered by lack of information regarding hard microdomain Tg and the heat capacity change at Tg (67, 68). Direct assessment of microdomain structure has been also attempted by electron microscopy, but with limited success, due to the difficulty in imaging individual microdomains of such small sizes in the range of tens of nm (69).

Based on these observations, several models which describe the two phase morphology have been proposed. Bonart et al, from wide angle x-ray diffraction (WAXD) and SAXS measurements, proposed that the hard segment units are ordered laterally in order to maximize inter-urethane hydrogen bonding (70-72). The hard segment sequences were assumed to exist in rigid, extended configurations within lamellar or sheetlike microdomains. This model was supported by further evidence from Blackwell and co-workers (73-75). Their WAXD results indicated that hard segment crystal thickness correlated well with the average hard segment molecular weight. However, the results of other SAXS studies were shown to be inconsistent with the rigid hard segment model (76, 77). The hard microdomain thicknesses in these works did not scale linearly with the average hard segment contour length. It was concluded that hard segment chains must be present in either coiled or folded configurations. Based on these observations, a lamellar model for hard microdomain structure was developed, where the hard microdomain thickness is controlled by the hard segment solubility within the soft microphase (77). Therefore, the hard microdomain thickness is approximately equivalent to the contour length of the shortest hard segment sequence which is insoluble in

the soft microphase. The longer sequences would then adopt non-rigid configurations, allowing reentry into hard microdomains for packing purposes.

In general, it has been found that the microstructure of polyurethanes consists of a lamellar or pseudolamellar composite of the hard and soft phases, with an average size on the order of 10 nm (78). An interfacial region which exist between these domains can be sharp or range up to a few nanometers. Also the phases are impure, that is, a significant fraction of the hard segments are dissolved in or reside within the soft phase. To a lesser extent, some mixing of the soft segments in the hard domains occur. In addition to microphase domain structure, a spherulitic superstructure can be seen in some systems with a high hard segment content where the hard segments are crystallizable (79).

## 2 - 3. Polymer Blends

In recent years, polymer blends have become an important area of research due to their growing versatility and commercial acceptance. This section will briefly summarize the fundamental concepts of thermodynamics of polymer-polymer miscibility followed by methods of miscibility determination and some examples of thermoplastic polyurethane blends. The term miscibility will be referred to as thermodynamic solubility of two components in the molecular level, while compatibility will be used in the sense of usefulness of the blend.

### 2 - 3 - 1. Basic Thermodynamics

The state of miscibility of two components is governed by the free energy of mixing, $\Delta G_{mix}$, which is defined by:

$$\Delta G_{mix} = \Delta H_{mix} - T\Delta S_{mix} \tag{1}$$

where $\Delta H_{mix}$ is the enthalpy change on mixing and $\Delta S_{mix}$ ,the entropy of mixing. The possible ways in which the free energy of mixing can vary with the composition of the overall mixture, where $\phi_i$ = volume fraction of component $i$ are shown in figure 9 (80). In case A, free energy of mixing is always positive indicating immiscibility of the components with each other. The opposite occurs for case B where free energy is always negative and the components are miscible in all proportions. But negative free energy does not insure complete misciblity as suggested by case C, where $\Delta G_{mix}$ shows a reversed curvature in the mid-composition range. In this range, the mixture can attain even lower free energy by splitting into two phases with compositions given by the two minima of the curve, resulting in a miscibility gap or partial miscibility. Therefore, a more complete criteria for thermodynamic miscibility would be to satisfy the following equation over the range of concentration (81):

$$\left[ \frac{\partial^2 \Delta G_{mix}}{\Delta \phi_2^2} \right]_{T,P} > 0 \qquad (2)$$

Since no direct measurement of free energy can be carried out, the terms in equation (1) must be estimated using thermodynamic models. The simplest model for polymer-polymer mixture is the Flory-Huggins lattice model (82). The theory estimates the entropy of mixing as the combinatorial contribution computed from the number of ways that the solvent and polymer molecules can be arranged in a lattice of fixed volume. The result of lattice analysis gives the following expression for entropy of mixing:

$$\Delta S_{mix} = \frac{-RV}{V_r} \left[ \frac{\phi_1 \ln \phi_1}{X_1} + \frac{\phi_2 \ln \phi_2}{X_2} \right] \qquad (3)$$
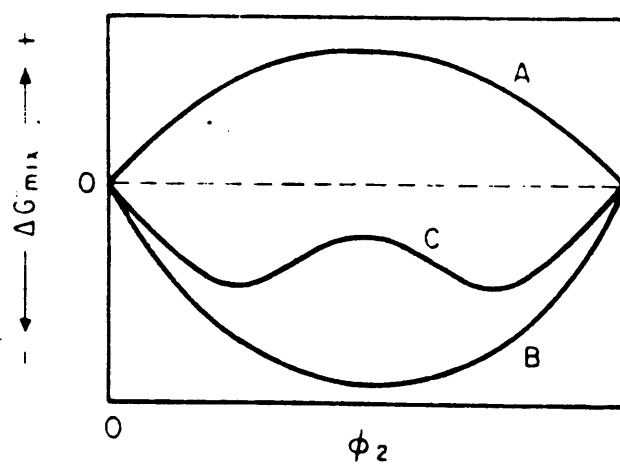
Figure 9. Free energy of mixing vs composition curve

where R is the gas constant, $V_r$ is a reference volume, and $X_i$ is the degree of polymerization of component i relative to the reference volume and is of the same order as the degree of polymerization expressed in terms of the number of monomer units in the chain.

It is important to note that the entropy change for mixing two high molecular weight polymers is dramatically less than that of two low molecular weight species. This is due to restrictions imposed on mixing by the connectivity of polymer chain which reduce the number of possible arrangements in the lattice. Thus, in the limit of very high molecular weights, the combinatorial entropy of mixing is essentially zero.

The enthalpy of mixing, on the other hand, is primarily dependent on the energy change associated with nearest neighbor contacts during mixing and not very dependent upon molecular lengths. In the case of mixing two polymers which only interact through dispersion or Van der Waals type forces, the heat of mixing can be adequately predicted from the solubility parameter of the components, $\delta$, using:

$$\Delta H_{mix} = V(\delta_1 - \delta_2)^2 \phi_1 \phi_2 \tag{4}$$

where V is the volume of the mixture (83). This equation always predicts a positive enthalpy of mixing or at best zero when the solubility parameters of the components are equal. Thus, miscibility is predicted to be a highly unlikely event and to promote miscibility, structural similarity of the components must be sought.

Many polymer pairs which does not meet the above criteria have been found to be miscible (84). The mechanism responsible for polymer-polymer miscibility are attributed to specific interactions between polymer components which result in negative heat of mixing. Interactions such as hydrogen bonding, charge transfer and ionic interactions have been found to promote miscibility.

To predict the enthalpy of mixing arising from specific interactions, Flory-Huggins interaction parameter, $\chi_{12}$, is defined as:

$$\chi_{12} = \frac{ZW_{12}R_1}{kT} \tag{5}$$

where Z is the coordination number, W is the increase in energy when new contact is formed between segments 1 and 2, k is the Boltzmann's constant, and r is the number of repeat unit segments in molecule 1 (82). The Chi parameter measures the degree of specific interaction between the mixed components and when it assumes a negative value, the enthalpy of mixing becomes negative according to the expression:

$$\frac{\Delta H_{mix}}{V} = \frac{\chi_{12}RT\phi_1\phi_2}{V_1} \tag{6}$$

where $V_1$ is the molar volume of component 1. Since the combinatorial entropy term approaches zero for high molecular weight polymer blends, the free energy of mixing depends only upon the enthalpic term. Therefore, when Flory-Huggins interaction parameter is negative, the Gibb's free energy term is also negative, indicating thermodynamic miscibility.

## 2 - 3 - 2. Methods of Determining Polymer-Polymer Miscibility

Various techniques have been developed to characterize and determine miscibility in polymer blends. The most common methods include thermal and mechanical testing, microscopy, and scattering techniques.

The glass transition temperature of the polymer measures the degree of segmental motion within the chain and is dependent on the chain environment. Hence, Tg is a useful criteria in determining miscibility (82, 84). The glass transitions have been studied using differential scanning calorimetry (DSC), and dynamic mechanical or dielectric relaxation methods. The latter techniques are usually more sensitive in detecting transitions. If the blend is

miscible on the molecular scale and form a single homogeneous, amorphous phase, it will show a single, sharp Tg intermediate between Tg's of the constituents. For immiscible blends, two distinct Tg's corresponding to each component are detected. In the case of partial miscibility, two possibilities exist. A broad transition region can occur indicating microheterogeneity of the system, where a distribution of compositions exist with a dispersion maximum occuring between those of the constituents. On the other hand, two Tg's which are shifted closer together can be detected indicating that each phase contains a certain concentration of the other component of the blend. When the blend constituents have very similar Tg's, this technique is not very useful in determining miscibility.

Even blend systems which exhibit single glass transition, thus considered miscible by above criteria, can show two phase heterogeneous morphology under microscopic techniques. The size and distribution of the dispersed phases in polymer blends have been studied using transmission electron microscopy (TEM), scanning electron microscopy (SEM), and phase contrast light microscopy (85). The dispersed phase of sizes ranging from 50 to 100 angstroms has been detected for different miscible systems where miscibility was considered to increase with decreasing size of the dispersed phase.

A crude but common criteria used for miscibility is optical transparency of the polymer film (84). Miscible blends give clear transparent films with inherent mechanical integrity while immiscible blends usually result in white opaque films without any mechanical strength. Such results are very inconclusive since transparency can ocurr due to similar refractive indices of the polymer constituents rather than miscibility of the polymers.

The scattering techniques (84) have been successfully used to characterize polymer-polymer miscibility. Small angle neutron scattering (SANS) can elucidate the chain conformation of the polymer mixtures. The local order of the polymer chains can be studied by means of electron and Rayleigh-Brillouin scattering, whereas the morphology can be studied from light scattering and small angle X-ray scattering (SAXS). The cloud point technique can measure the temperature at which the blend changes from transparent homogeneous state

to cloudy inhomogeous state. The cloud point curves are generated as a function of temperature and blend composition.

Other methods employed include melting point depression and Fourier Transform Infared Spectroscopy (FTIR). For blend systems which contain a crystallizable component, the decrease in the melting point indicates the degree of miscibility due to the disruption of crystallinity as a result of phase mixing (85). FTIR is used to study the types of molecular interactions which are responsible for the polymer-polymer miscibility (87, 88).

## 2 - 3 - 3. Thermoplastic Polyurethane Blends

Blending of polymeric materials has become an important technological process in the last decades as a method of improving physical properties of the material. The first thermoplastic urethane (TPU) blends studied were alloy systems based on polyurethane (synthesized from polycaprolactone or polytetramethylene oxide, MDI, and butanediol) and various polymers such as polyvinyl chloride (PVC), acrylonitrile-butadiene-styrene terpolymer (ABS), and styrene-acrylonitrile copolymer (SAN) (89). Mechanically compatible blends were obtained with urethane elastomer contributing property improvements in the areas of wear resistance, toughness, low temperature flexibility, and resistance to hydrocarbons, oxidation and ozone. The other polymer components imparted increased stiffness and higher initial modulus to polyurethane.

Subsequently, similar investigations of TPU blends with polystyrene, SAN, polyhydroxy ether (Phenoxy A), and poly(vinyl ethyl ether) has been carried out (90). The polyurethane elastomer was based on polycaprolactone diol with approximately 2100 g/mol number average molecular weight, MDI, and butanediol. Two separate glass transitions obtained for blends of TPU with polystyrene, SAN and poly(vinyl ethylether) demonstrated the immiscibility of these systems. However, the mechanical properties obtained were intermediate between the constituents. An increase in the amount of urethane polymer in the blend resulted in re-

duced material stiffness, but increased elongation and rupture energy. These systems were considered mechanically compatible. The blends of Phenoxy A and the TPU exhibited miscibility based on the appearance of a single glass transition temperature which was dependent on the respective concentration of the components.

In the study of blends of PVC with polyurethanes, better impact strength and processibility, but lower thermal stability were observed (91, 92). All systems were immiscible. In another study, the interaction between PVC molecules and the hard segments of polyurethanes dispersed in soft segment regions were reported (93). Morphological models for specimens cast from solutions of different solvents were suggested. The influence of soft segment structure on the morphology of TPU-PVC blends was also investigated (94, 95). The results indicate that it is possible to change the morphology of blends by changing the structure of the soft segments. The polyester soft segments were found to be more compatible with PVC than polyether ones. Blends of PVC with polycaprolactone based polyurethanes exhibited increased miscibility with increasing chain length of polycaprolactone (96).

Recent studies of polyurethane urea blended with polydimethylsiloxane indicated that total phase segregation occur between the two polymers (97). However, small amounts of polyurethane -b- polydimethyl siloxane block copolymer can be added to compatibilize the two phases and the mechanical properties of the modified blends can be enhanced. In general, polyurethane blend systems are immiscible but mechanically compatible with other systems.

# Chapter III. EXPERIMENTAL

## 3 - 1. Introduction

The experimental procedures described in this chapter can be summarized in the following manner. The first step involves the synthesis of various amine terminated oligomers to be used as the soft segments for polyureas and polyurethane ureas. Three types are prepared: polydimethylsiloxane, poly(dimethyl-diphenyl)siloxane, and polypropylene oxide (PPO). In the second step the prepared oligomers and the commercial oligomers of polypropylene oxide (Jeffamine) and polytetramethylene oxide (PTMO) (DuPont) were used to synthesize polyureas and polyurethane ureas.

The characterization of these three groups of materials was then conducted. The systems included polyether ureas (with various soft segments); blends of polysiloxane ureas with polyether urea (based on Jeffamine soft segment); and siloxane incorporated polyether urea (based on Jeffamine) and polyurethane urea (based on PTMO).

## 3 - 1.  Synthesis of Polysiloxane Oligomers

### 3 - 1 - 1.  Reagents

Tetramethylammonium hydroxide pentahydrate was purchased from Aldrich. Octamethylcyclotetrasiloxane ($D_4$) and octaphenylcyclotetrasiloxane ($D_4''$) were supplied by General Electric and Union Carbide. 1,3-bis ($\gamma$-aminopropyl) tetramethyldisiloxane (DSX) was obtained from Petrarch Chemicals.  All reagents were used as received.

### 3 - 1 - 2.        Aminopropyl Terminated Polydimethylsiloxane

Based on the desired average molecular weight of the oligomer, calculated amounts of $D_4$ and DSX end blocker were added into a three-necked round bottom flask fitted with an overhead mechanical stirrer, a nitrogen inlet, and a condenser with a drying tube.  0.5 wt. percent of the siloxanolate catalyst was charged into the flask and the equilibration reaction was caried out at 80 °C for 48 hours in a silicon oil bath.  To decompose the catalyst, the mixture was reacted for additional 3 hours at 150 °C.  The resulting product was vacuum stripped for 4 hours at 250 millitorrs and 120 °C.  Approximately 10 wt.% of cyclics were stripped off.  The siloxane oligomers prepared are shown in Table 4.  The molecular weights were obtained by end group titration method which is described in latter section.

The siloxanolate catalyst was prepared in bulk by heating $D_4$ and tetramethylammonium hydroxide pentahydrate in ten to one mole ratio at 75 °C for 24 hours.  The apparatus consisted of a flask equipped with a nitrogen inlet, an overhead mechanical stirrer, and a dean stark trap with a condenser.  The catalyst was stored in a dessicator until needed.

Table 4. Polysiloxane oligomers

| TYPE* | TARGET <Mn> | TITRATED <Mn> |
|-------|-------------|----------------|
| PSX   | 1000        | 1150           |
| PSX   | 2000        | 2200           |
| PSX   | 5000        | 5000           |
|       |             |                |
| p-PSX | 2000        | 2600           |
| p-PSX | 5000        | 5300           |
| p-PSX | 10000       | 11700          |

\*   PSX : Polydimethylsiloxane
    p-PSX : Poly(dimethyl-diphenyl) siloxane with 50 wt%
         diphenyl units

### 3 - 1 - 3.    *Aminopropyl Terminated Poly(dimethyl-diphenyl)siloxane*

According to the desired molecular weight of the product and the level of diphenylsiloxane units, calculated amounts of $D_4$ , $D_4''$, and DSX were introduced into the reaction set up described above for the polydimethylsiloxane oligomer.  After adding 0.2 mole percent of the siloxanolate catalyst, reaction was allowed to proceed for 72 hours at 80 °C, followed by additional 3 hours at 150 °C to decompose the catalyst.  After 36 hours, the mixture turned homogeneous as the diphenyl units are incorporated into the polymer chain.  The product mixture was vacuum stripped for 4 hours at 100 millitorrs and 200 °C to remove the cyclics.  The resulting product was a clear viscous liquid. The oligomers prepared are shown in Table 4 and theoretically contain 50 wt. percent of diphenyl units in the chain.

### 3 - 1 - 4.  *Amine Terminated Polypropylene Oxide*

Detailed procedure for the synthesis of amine terminated polypropylene oxide oligomers is described elsewhere (98).  The polymerization was carried out by reacting nitro phenol modified aluminum porphyrin catalyst with propylene oxide monomer, followed by coupling the secondary hydroxyl group ends of the oligomer chain with terephthaloyl acid chloride to obtain difunctional nitro-terminated oligomers.  The reaction scheme is outlined in figure 10. The nitro group is then reduced by hydrogenation at 45 psi of hydrogen pressure in the presence of Pd/C catalyst for 24 hours.  The number average molecular weight of the oligomers was 2000 and 2800 g/mol, as determined from end group titration.

Figure 10. Reaction scheme for PPO oligomer synthesis
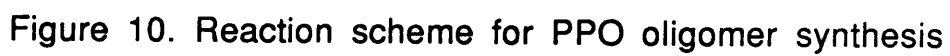
# 3 - 2. Synthesis of Polyurea Segmented Copolymers

## 3 - 2 - 1. Reagents

4,4-methylene diphenylisocyanate (MDI) from KODAK was vacuum distilled and stored in a dessicator at 0 °C prior to use. Ethylenediamine (ED) from Aldrich was distilled over calcium hydride and stored in a dessicator. The solvents used were tetrahydrofuran (THF) which was dried over calcium hydride for 24 hours, then distilled before use, and N,N dimethylacetamide (DMAC) which was dried over phosphorous pentoxide then distilled under reduced pressure. Both reagents were purchased from Fisher.

## 3 - 2 - 2. Polysiloxane-ureas

The reaction apparatus consisted of a round bottom, three- necked flask fitted with an addition funnel, an overhead mechanical stirrer, a nitrogen inlet, and a condenser with a drying tube. The same set-up was utilized for all the following reactions.

Equimolar amounts of MDI and aminopropyl terminated polysiloxane oligomers were dissolved in THF separately. After purging the reaction flask with nitrogen for an hour, the isocyanate solution was transferred to the flask and the polysiloxane solution was added dropwise via the addition funnel. The reaction was carried out at room temperature for three to four hours, until the disappearance of the isocyanate absorption band from the FTIR spectra was verified. The reaction scheme for the siloxane-urea synthesis is outlined in figure 11. The concentration of the solution was 15 wt./vol percent of solids. The viscosity of the solution increased gradually as the molecular weight of the polymer increased, as expected.

The polymers obtained were coagulated in 50/50 volume ratio of methanol/water mixture, filtered and washed with methanol several times. The product was dried in vacuum oven

Table 5. Polysiloxane urea segmented copolymers

| SOFT SEGMENT SILOXANE OLIGOMER | | | HARD SEGMENT MDI |
| --- | --- | --- | --- |
| TYPE* | <MN> | Wt% | Wt% |
| PSX | 1150 | 82.1 | 17.9 |
| PSX | 2200 | 89.8 | 10.2 |
| PSX | 5000 | 95.2 | 4.8 |
| p-PSX | 2600 | 91.2 | 8.8 |
| p-PSX | 5300 | 96.5 | 4.5 |
| p-PSX | 11700 | 97.9 | 2.1 |

*  PSX  :  Polydimethylsiloxane
   p-PSX  :  Poly(dimethyl-diphenyl)siloxane with 50 wt%
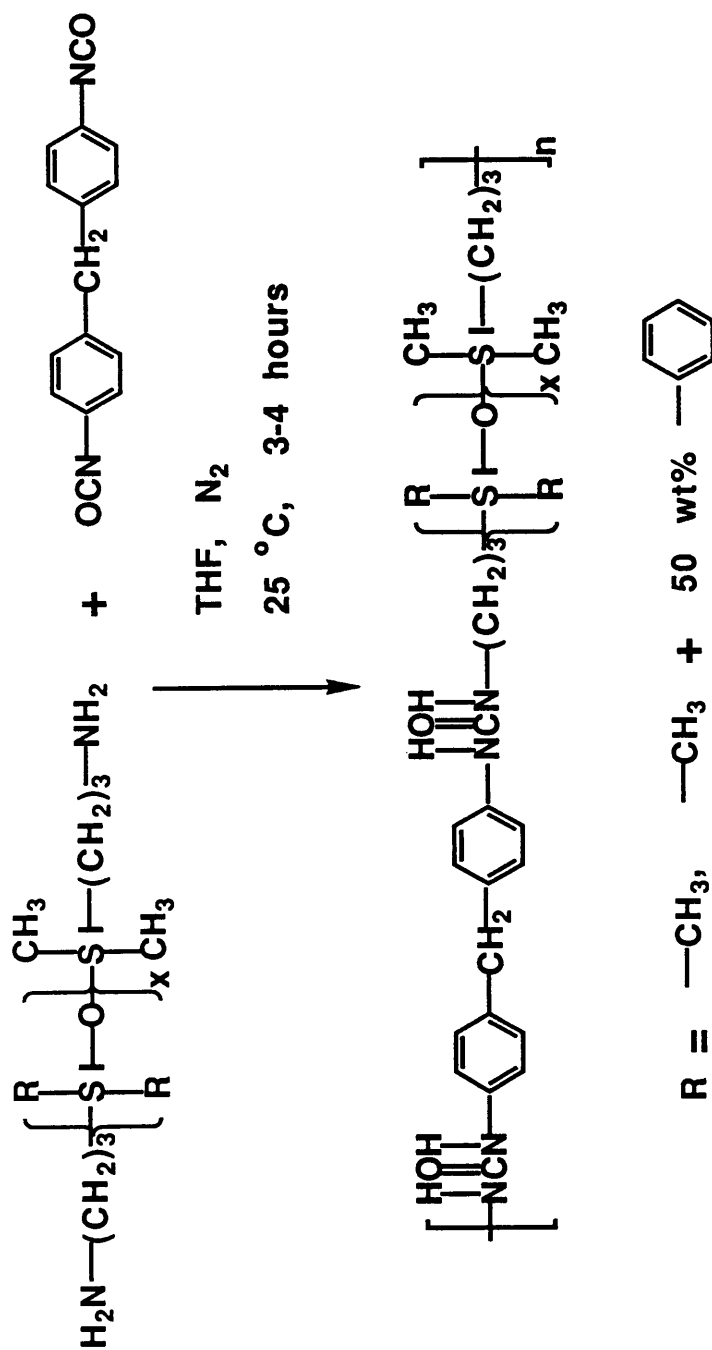            diphenyl units

Figure 11. Reaction scheme for Polysiloxane urea synthesis

for 36 hours at 80 °C.  This work up procedure was repeated twice and was used for all the polymers synthesized.  The siloxane-urea polymers prepared are listed in Table 5.


### 3 - 2 - 3.  Polypropylene oxide-ureas


Both commercial polypropylene oxide (Jeffamine) and oligomers prepared from this laboratory (PPO) were used as soft segment polyether diamine.  The oligomers were dehydrated at 70 °C under vacuum for 24 hours prior to use.

As illustrated in figures 12 and 13, the synthesis of polyureas were carried out by a two step process:  First, MDI was weighed into the reaction flask and dissolved in DMAC.  Then a solution of oligomer in DMAC was added dropwise to form an isocyanate capped prepolymer.  At this stage, the viscosity of the solution did not increase significantly due to the fairly low molecular weight of the prepolymer.  In the second step, a solution of ethylenediamine in DMAC (1 v/v percent) was added dropwise via an additional funnel to ensure correct stoichiometry.  This was necessary for better control over the fast the fast isocyanate- amine reaction.  A gradual increase in the solution viscosity of the mixture was observed upon the addition of chain extender as expected.

The reaction was allowed to proceed for 3 - 4 hours at room temperature, to minimize the side reactions which can lead to branching and even crosslinking.  The solids content in the solution was 7 - 15 wt./vol percent and solution remained homogenous throughout the reaction.  The hard segment content was 20 wt. percent relative to the total reactants and consisted of MDI and ethylenediamine chain extender.  The prepared polymers are listed in Table 6.

For polyureas with various siloxane segments incorporated in the polymer backbone, a similar procedure to that described above was utilized.  The oligomer was composed of a mixture of Jeffamine and polysiloxane in solution which was then added to the isocyanate solution via an addition funnel.  Poly (dimethyl-diphenyl) siloxanes formed clear homogeneous mixtures with Jeffamine in DMAC and remained miscible throughout the reaction.
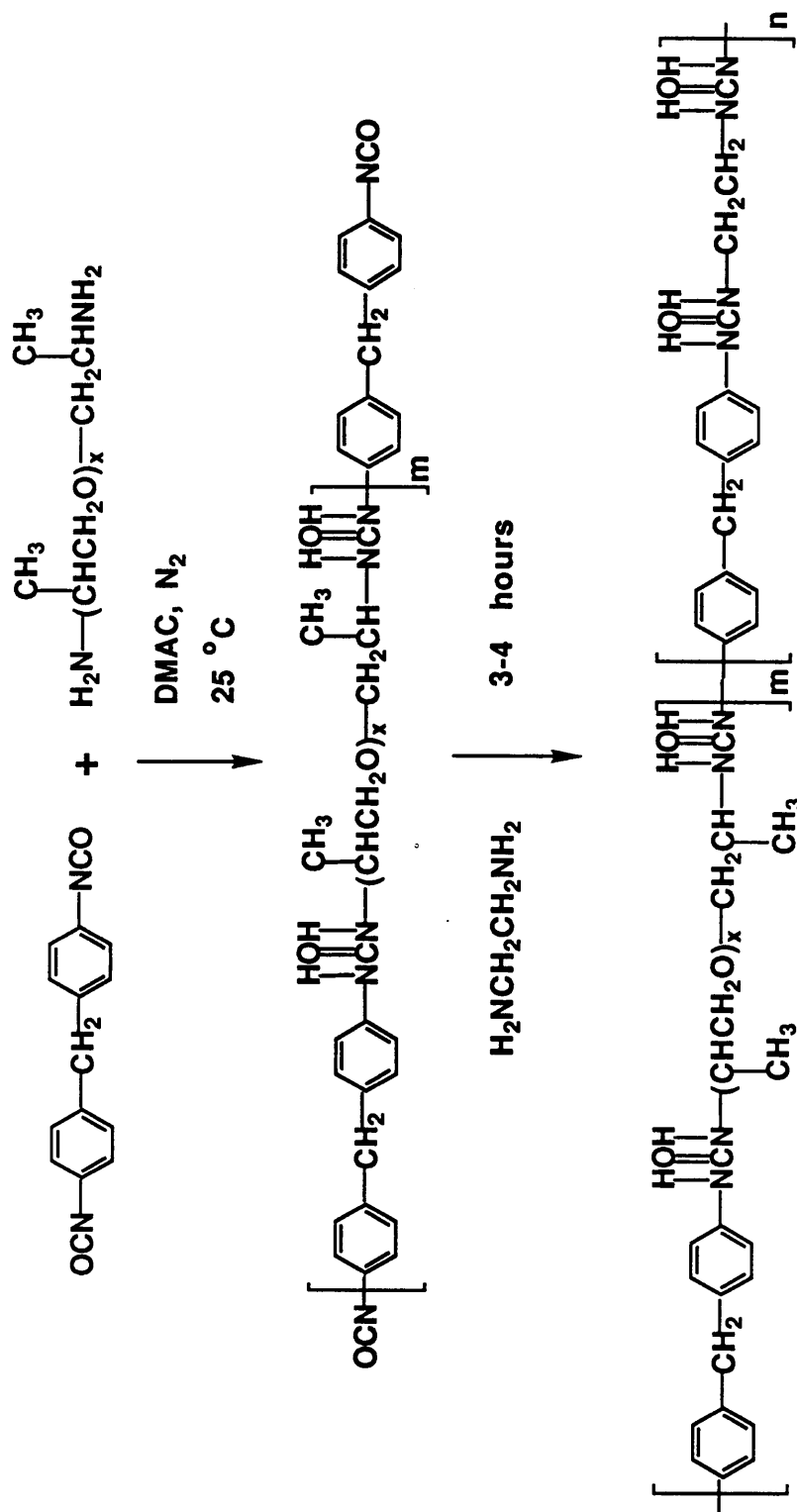
Figure 12. Reaction scheme for commercial Jeffamine polyol-urea segmented copolymer synthesis
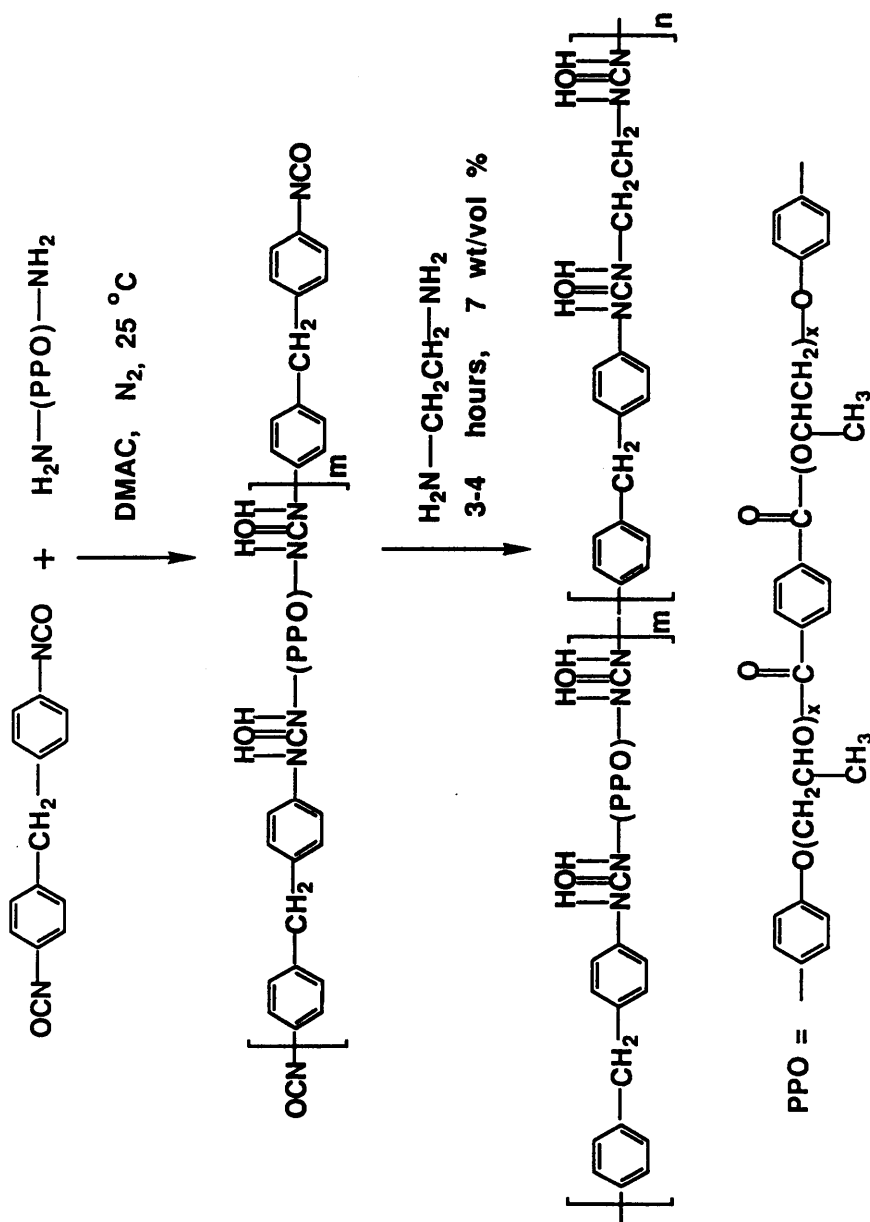
Figure 13. Reaction scheme for difunctional aminophenyl PPO urea segmented copolymer synthesis

Table 6. Polypropylene oxide urea segmented copolymers

| | SOFT SEGMENT POLYAMINE | | | HARD SEGMENT* | |
| | | | | MDI | ED |
| TYPE | <Mn> | Wt% | | Wt% | Wt% |
|---|---|---|---|---|---|
| JEFFAMINE | 2000 | 80.0 | | 18.1 | 1.9 |
| PPO | 2000 | 80.0 | | 18.1 | 1.9 |
| PPO | 2800 | 80.0 | | 17.5 | 2.5 |

* Hard segment : soft segment = 20 : 80 (wt%)

Polydimethylsiloxanes were immiscible with Jeffamines in DMAC and varying amounts (10 to 50 vol percent) of THF co-solvent were tried. This resulted in a clear prepolymer solution, but became inhomogeneous during the chain extension step in most cases. An exception was the experiment using polydimethylsiloxane with molecular weight of 1150 g/mol, where incorporation of 8 percent by weight of polydimethylsiloxane was possible using DMAC/THF (80/20 vol. ratio) co-solvents. Only those compositions which resulted in a clear homogeneous mixture throughout the reaction was considered for further characterization (Table 7).

## 3 - 3. Synthesis of Polyurethane-urea Segmented Copolymers

Hydroxyl terminated polytetramethylene oxide (PTMO), with the molecular weight of 2000 g/mol., obtained from DuPont was used as soft segment. The oligomer was dried at 70 °C under vacuum for 24 hours before use. Tin octoate catalyst from Pfaltz & Bauer, Inc. was used as received.

Similar reaction procedures as those described above were followed (Figure 14). Thus, MDI was weighed into the reaction flask and dissolved in dry DMAC, followed by the addition of PTMO oligomer solution in DMAC. The mixture was heated to 50 °C and approximately 0.1 wt.percent of the tin octoate catalyst was added. Higher temperature and catalyst were used to increase the reaction rate of hydroxyl end groups, which are much slower reacting than amine end groups with the isocyanate. After an hour, the reaction was cooled to room temperature and ethylenediamine solution was added dropwise. The mixture was reacted for 3 - 4 hours, which produced a viscous homogeneous solution.

For siloxane incorporated polyurethane-ureas, the same procedure was followed. The oligomer solution was composed of PTMO and varying amounts of polydimethylsiloxane in DMAC/THF (60/40 volume ratio) co-solvents. Due to the fast reaction of amine end groups with isocyanates, it was possible that the siloxane oligomer formed a high molecular weight species before the hydroxyl end groups of PTMO could react with isocyanates. However, a

Table 7. Siloxane incorporated Jeffamine-urea segmented copolymers

| | SOFT SEGMENT* | | | HARD SEGMENT | |
| | POLYSILOXANE | | JEFFAMINE** | MDI | ED |
| TYPE* | \<Mn\> | Wt% | Wt% | Wt% | Wt% |
|---|---|---|---|---|---|
| PSX | 1150 | 8.0 | 72.0 | 18.3 | 1.7 |
| p-PSX | 2600 | 8.0 | 72.0 | 18.0 | 2.0 |
| p-PSX | 2600 | 16.0 | 64.0 | 18.0 | 2.0 |
| p-PSX | 2600 | 24.0 | 56.0 | 17.9 | 2.1 |
| p-PSX | 5300 | 8.0 | 72.0 | 17.9 | 2.1 |
| p-PSX | 5300 | 16.0 | 64.0 | 17.8 | 2.2 |
| p-PSX | 5300 | 24.0 | 56.0 | 17.7 | 2.3 |

*PSX : Polydimethylsiloxane
  p-PSX : Poly(dimethyl-diphenyl)siloxane with 50 wt% diphenyl
          units
**Jeffamine : 2000 g/mole
  Hard segment : Soft segment = 20 : 80 (Wt%)
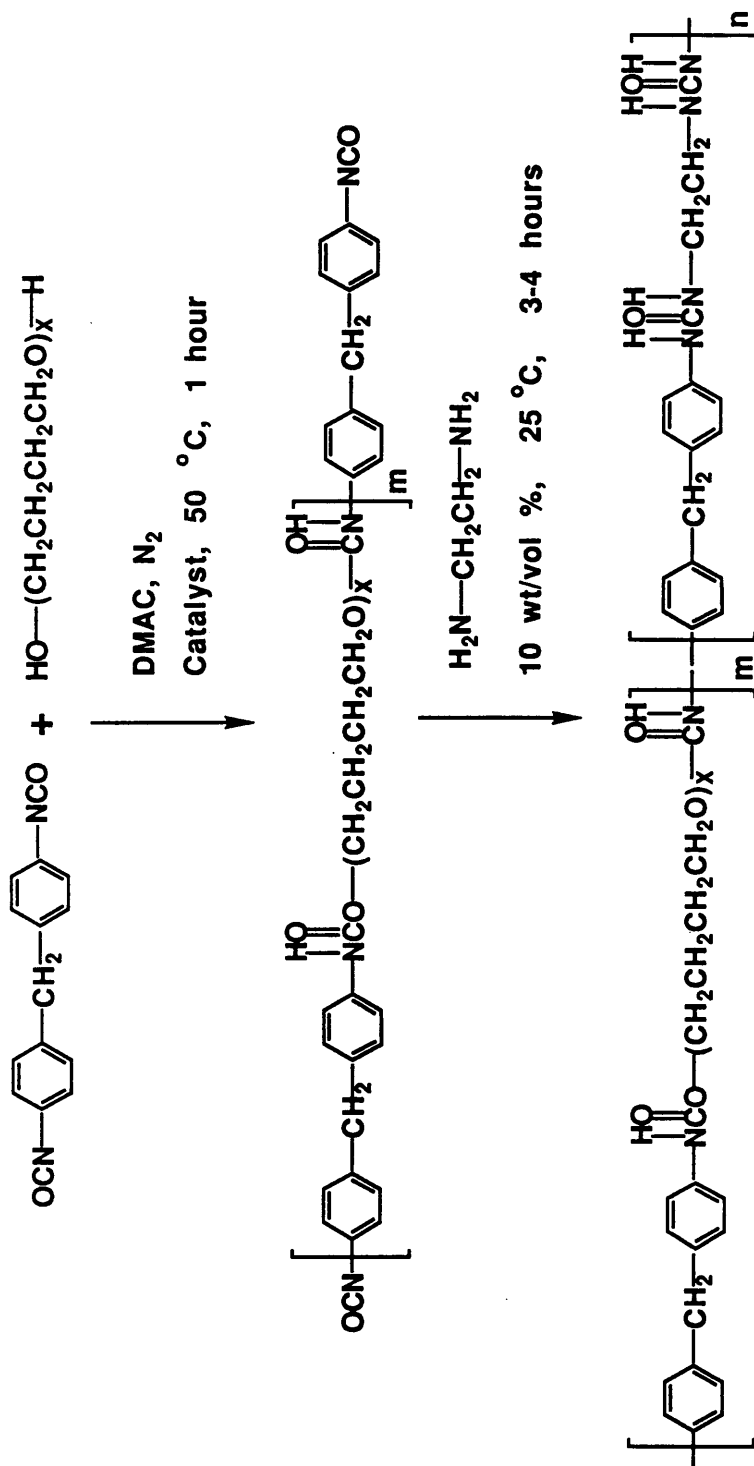
Figure 14. Reaction scheme for polyurethane urea segmented copolymer synthesis

significant viscosity increase was not observed during the prepolymer stage. In the cases where the mixtures of PTMO and polydimethylsiloxane oligomers were immiscible, the solvent ratio of DMAC and THF were varied. But the solution became inhomogeneous in either prepolymer stage or during the chain extension step. The solids content of the solution was maintained at 10 wt./vol. percent and the hard segment content was 20 wt. percent of the total reactants. Only those compositions of oligomers which remained homogeneous throughout the reaction were selected for further analysis (Table 8).

## 3 - 4. Preparation of Blends

Blends of polypropylene oxide-urea (based on Jeffamine with 2000 molecular weight) and various polysiloxane-urea segmented copolymers were prepared by dissolving calculated amounts of each component in DMAC solvent at 10 wt./vol percent concentrations. Those solutions which were transparent were cast on to a clean glass plate and dried under IR lamp at 65 to 70 °C for 12 hours, then placed in the vacuum oven for 36 to 48 hours at 80 °C. The blend systems for further analysis were chosen based on the clarity of the solution mixture and the solvent cast films.

## 3 - 5. Characterization

### 3 - 5 - 1. Sample Preparation

The polymer samples were dissolved in an appropriate solvent at 10 to 15 wt./vol percent concentrations. The solution was then poured on to a clean glass plate and dried based on the type of solvent used. For polysiloxane-urea copolymers dissolved in THF, the solvent was

Table 8. Siloxane incorporated polyurethane urea segmented copolymers

| SOFT SEGMENT | | | HARD SEGMENT* | |
| POLYDIMEHTYLSILOXANE | | PTMO** | MDI | ED |
| <Mn> | Wt% | Wt% | Wt% | Wt% |
| --- | --- | --- | --- | --- |
| - - | - - | 80.0 | 18.1 | 1.9 |
| 1150 | 8.0 | 72.0 | 18.2 | 1.8 |
| 1150 | 16.0 | 64.0 | 18.3 | 1.7 |
| 1150 | 24.0 | 56.0 | 18.5 | 1.5 |
| 2200 | 8.0 | 72.0 | 18.1 | 1.9 |
| 2200 | 16.0 | 64.0 | 18.0 | 2.0 |
| 2200 | 24.0 | 56.0 | 18.0 | 2.0 |

* Hard segment : Soft segment =  20 : 80 Wt%
** PTMO :  <Mn> = 2000 g/mole

allowed to evaporate at room temperature for 24 hours, then dried in vacuum oven at 70 °C for 24 hours.  For other samples which were dissolved in a high boiling solvent like DMAC, the polymer film was dried under IR lamp at 60 to 70 ° C for 12 hours, then in a vacuum oven at 80 ° C for 36 to 48 hours.  The films were peeled from the plate and stored in a dessicator until needed for physical testing.

## 3 - 5 - 2.  *Titrations*

The number average molecular weights of the oligomers were determined by potentiometric titration of the functional end groups using a Fisher Scientific Titrimeter II.  The oligomers were weighed into a 250 ml beaker and dissolved in 100ml of equal volume mixture of isopropanol and tetrahydrofuran.  The standard titrant of 0.1N HCl in isopropanol (Fisher) was used to titrate the amine end groups.  A blank titration of the solvent was performed prior to the titration of the oligomer.  The number average molecular weight of the oligomer was calculated from the following equation:

$$<Mn> = \frac{(\text{sample weight}) \times (\text{number of functional end groups})}{(\text{equivalent of titrant at end point})}$$

An average of three titrations were performed for each sample.

## 3 - 5 - 3.  *Fourier Transform Infrared Spectroscopy (FTIR)*

The chemical structures of the polymer were confirmed by FTIR spectra obtained from Nicolet MX-1 spectrometer.  The samples were solvent cast (DMAc) onto the salt plate and dried in the vacuum oven for two hours at 70 °C to form a thin film.

### 3 - 5 - 4. Intrinsic Viscosity

Intrinsic viscosity measurements were carried out using a Cannon - Ubbelhode viscometer placed in a thermostatic water bath at 25 °C. Generally three flow times were measured from a solution of 0.1 grams in 25 ml of DMAC or THF. This process was repeated for three different dilutions of the same sample. The intrinsic viscosity value was determined from the intercept of specific viscosity of each concentration.

### 3 - 5 - 5. Differential Scanning Calorimetry (DSC)

The glass transition temperatures and melting transitions of the polymer were determined by Perkin-Elmer Model DSC-2 instrument Both the first and second runs were recorded at 10 °C/min heating rate, in the temperature range of -130 °C to 250 °C. Subambient measurements were made by cooling the system with liquid nitrogen while the sample chamber was purged with helium.

### 3 - 5 - 6. Thermogravimetric Analysis (TGA)

The thermal stability of the copolymers was studied from weight loss measurements using a Perkin-Elmer TGS-2 instrument. Dynamic thermograms were obtained at a heating rate of 10 °C/ min under nitrogen or air atmosphere (20 cc/min.) from 0 °C to 800 °C.

### 3 - 5 - 7. Thermomechanical Analysis (TMA)

Thermomechanical analysis was performed with a Perkin-Elmer Thermal Mechanical Analyzer. The extent of penetration was measured under a 10 gram of load at the heating rate

of 10 °C/min. under nitrogen flow of 20 cc/min. Temperature range of -150 °C to 250 °C was covered.

### 3 - 5 - 8. Stress Strain Analysis

Uniaxial stress-strain test was performed by Instron Model 1123 at room temperature at a crosshead speed of 0.5 in/min. Dog bone specimens were punched out from the solvent cast films using a die with a gauge length of 10 mm. The tensile strength data reported are based on the maximum stress at break obtained from the average of five to ten specimens tested. The hysteresis of the selected samples was measured from the area under the stress strain curve which was obtained by uniaxially stretching the sample at a crosshead speed 0.5 in/min up to 800 percent elongation, then unloading at the same crosshead speed. The difference in the area under the loading and unloading curve was calculated. A minimum of four samples were tested.

### 3 - 5 - 9. X-ray Photoelectron Spectroscopy (XPS)

The surface composition of the polymer samples was determined using the KRATOS XSAM 800 XPS system. The samples were solvent cast onto a rectangular strip (0.8 cm.x1.5 cm.) of a ferrotype plate and dried under an IR lamp at 60 to 70 °C for 12 hours, then under vacuum at 80 °C for 36 hours. The metal strips on which the polymer films were cast were attached to the sample holder with a screw and inserted into the sample chamber.

The pressure in the sample chamber was maintained at approximately $10^{-9}$ torr during spectra collection. The x-ray source was magnesium anode, normally run at 13 kV and 20 mA. The analyzer was operated in the Fixed Retarding Ratio (FRR) mode. Narrow scans of the spectra were obtained using an analyzer slit width of 2 mm in order to detect fine features. The electron take-off angle between the analyzer and the sample surface was varied

from 90° to 10° to change the sample depth from 50 - 60 angstroms to 10 angstroms of the top layer.

# Chapter IV. RESULTS AND DISCUSSION

Segmented polyureas and polyurethane ureas are thermoplastic elastomers produced by chemically joining two dissimilar polymer blocks along the chain backbone. At service temperatures one of the components is rubbery in nature (soft segment) while the other is a glassy or semicrystalline thermoplastic (hard segment). Due to incompatibility between the hard and soft components, these materials undergo microphase separation in the solid state. The resulting two-phase structure consists of aggregates or domains of hard segments dispersed in a soft segment elastomeric matrix.

The characterization data of these systems can be put into a proper framework by considering the propensity of the material to undergo this microphase separation. Soft segment chemical composition, molecular weight and degree of phase mixing control the low temperature $T_g$ of the system. The volume fraction of hard segment controls the modulus level, strength, and high temperature softening behavior, since the urea/urethane segments reside primarily in rigid domains which serve both as viscoelastic filler particles and physical crosslinks. Variation of these factors affect the quality of phase separation which influence physical properties of segmented polyureas and polyurethanes.

# 4 - 1. Synthesis

Segmented polyether urea (PEU) and polyether urethane urea (PEUU) copolymers were prepared by using the two-step solution polymerization technique. The endcapping or prepolymer stage of the two-step reaction is designed to convert the functional end groups of the soft segment to isocyanate (NCO) groups, and to produce an excess of free unreacted isocyanate in the reaction mixture. The second step or the chain extension step is designed to couple the isocyanate capped prepolymer and the unreacted isocyanates with ethylene diamine (ED) through urea formation. Since aliphatic diamines react very fast with isocyanates, the diamine solution was added slowly at room temperature under vigorous stirring. The reactants used were difunctional and a stoichiometric ratio of $NCO/NH_2$ or $NCO/(NH_2 + OH)$ was employed. An excess of NCO groups can react with already formed urea or urethane linkages, subsequently leading to chemical crosslinking which was undesirable. Under these reaction conditions linear high molecular weight products are obtained.

A critical step in the polymer synthesis was the choice of a reaction solvents because of the differences in the solubility parameters of non-polar polyether and polar urea or urethane components. As the molecular weight increases during chain extension, more urea or urethane linkages are introduced. This necessitated the presence of polar organic solvents like DMAC to prevent premature precipitation of the polymer. In addition, fairly dilute concentrations, 10 wt/vol % or less, were utilized due to this solubility decrease and viscosity increase as the polymerization proceeded.

In the synthesis of PEUs containing polypropylene oxide (PPO) soft segment with MDI and ED hard segment, DMAC solvent was sufficient to obtain a homegeneous solution throughout the reaction. However, when polydimethylsiloxanes (PSX) were incorporated as a part of the soft segment together with commercial PPO (JEF), a cosolvent was needed to ensure the solubility of PSX which is immiscible in DMAC. It was found that a 1:4 ratio of THF to DMAC could be used satisfactorily to incorporate small amounts (8 wt %) of low molecular

weight (1150 g/mol) PSX in polyether ureas with 20 wt% hard segment content. However, at higher wt% incorporation or higher molecular weight PSX, this solvent mixture was insufficient to allow a homogeneous reaction mixture. Thus, in the prepolymer stage, more THF was needed to solubilize the polydimethylsiloxane and this reduced the polarity of the solvent mixture. As more urea linkages are formed during the chain extension step, the solvent mixture was not polar enough for the growing macromolecules and the solution became inhomogenous.

Thus, synthesis of polydimethylsiloxane incorporated polyether ureas was very limited due to large differences in the solubility parameters of the siloxane and urea components. This was less of a problem for the incorporation of poly(dimethyl-diphenyl) siloxane oligomers which are soluble in DMAC as a result of the more polar diphenyl substituents on the siloxane backbone. In the oligomer series studied, the reaction mixture in DMAC became inhomogeneous only for the case of high molecular weight (11700 g/mol) oligomer, which contain long sequences of polydimethylsiloxane.

In the synthesis of siloxane incorporated PEUUs, a 2:3 solvent ratio of THF to DMAC was utilized. Higher THF content was possible due to the lower amount of urea components. Since urethane components are less hydrogen bonded than urea components a less polar solvent mixture could be used. However, for higher molecular weight (5000 g/mol) polydimethylsiloxane, the incompatibility between the siloxane and hard segments of MDI and ED was too large at 20 wt% hard segment content and this resulted in an inhomogeneous reaction mixture. During the prepolymer stage, both the hydroxyl end groups of PTMO oligomer and amine end groups of polydimethylsiloxane oligomers were reacted with MDI, forming urethane and urea linkages, respectively. The latter reaction proceeds much faster than hydroxyl-isocyanate reactions which could result in high molecular weight siloxane urea chains before PTMO segment can react. Nevertheless, a major viscosity increase accompanying the molecular weight build-up was observed only during the chain extension step.

For polysiloxane urea segmented copolymers, stoichiometric amounts of siloxane oligomers and MDI were reacted in THF solvent. Even without the chain extender, large in-

compatibility between soft and hard segments exist resulting in microphase separated materials. Since the hard segments consisted only of short individual MDI units, they are much less hydrogen bonded than polyether ureas mentioned above. Therefore, less of the polar solvent like THF can be used for these perfectly alternating segmented copolymers at low hard segment content.

FTIR spectra were collected for materials synthesized which ensured that the polymerization was complete and that the desired structure was obtained. Typical spectra of polysiloxane urea and polyether urea copolymers are shown in Figure 15. The urea linkage is best characterized by the N-H and C=O absorption bands. The major N-H absorption band occurs at $3330 cm^{-1}$ while other amide absorptions are observed at 1530 and 1305 cm sup <-1>. The carbonyl absorption is split into two peaks at about 1730 and $1703 cm^{-1}$ which are assigned to free and hydrogen bonded carbonyl groups respectively. For PPO based polyureas, a strong absorption band of the C-O-C linkage at $1105 cm^{-1}$ can be distinguished, while a Si-O-Si stretch at $1065 cm^{-1}$ can be observed for polysiloxane ureas. The absence of a strong peak around $2250 cm^{-1}$ corresponding to isocyanate groups suggested that the copolymerization had reached high conversion.

The series of segmented polyurea and urethane urea copolymers prepared are listed in Table 9, along with their intrinsic viscosity data. Series I samples are based on amine terminated polydimethyl siloxane (PSX) and poly(dimethyl-diphenyl)siloxane (pPSX) soft segments and MDI hard segment. These specimens are designated "X<Mn> - MDIY", where X represents type of oligomer with number average molecular weight <Mn> and Y represents the weight percent of MDI hard segment. Series II samples were synthesized from amine terminated polypropylene oxide, both commercial material (JEF) and one synthesized in this laboratory (PPO). The hard segment of MDI and ethylene diamine chain extender comprised 20 wt% of the polymer and is represented as "H20".

Series III samples are classified as "UR-X<Mn>-Y", with UR denoting the control polyurea (JEF2000-H20) and Y showing the weight percent of polysiloxane, X<Mn>, incorporated into the control polymer. Similar nomenclature is employed for series IV specimens,
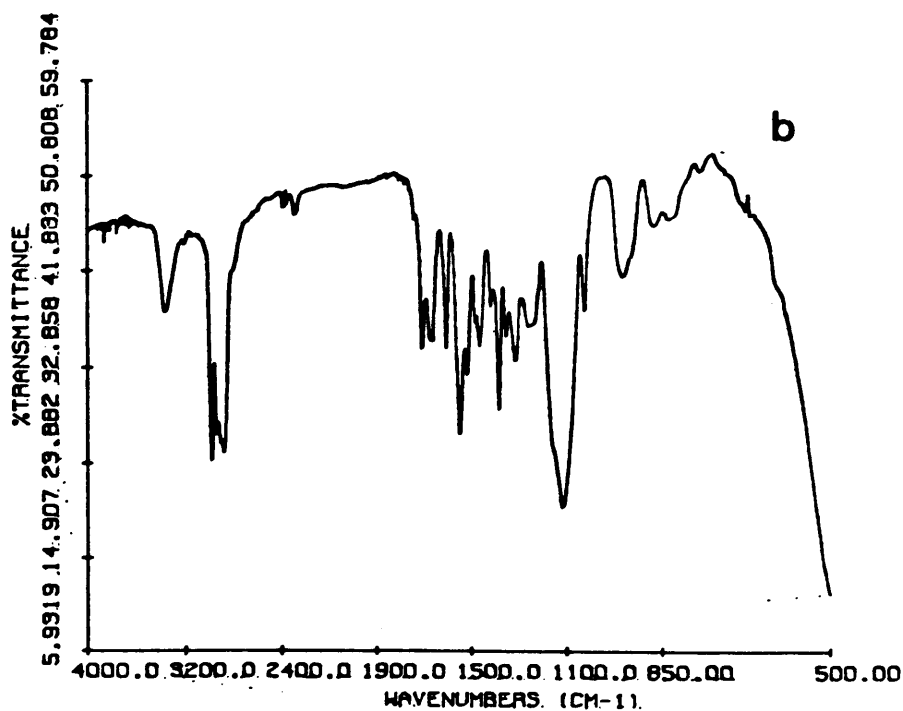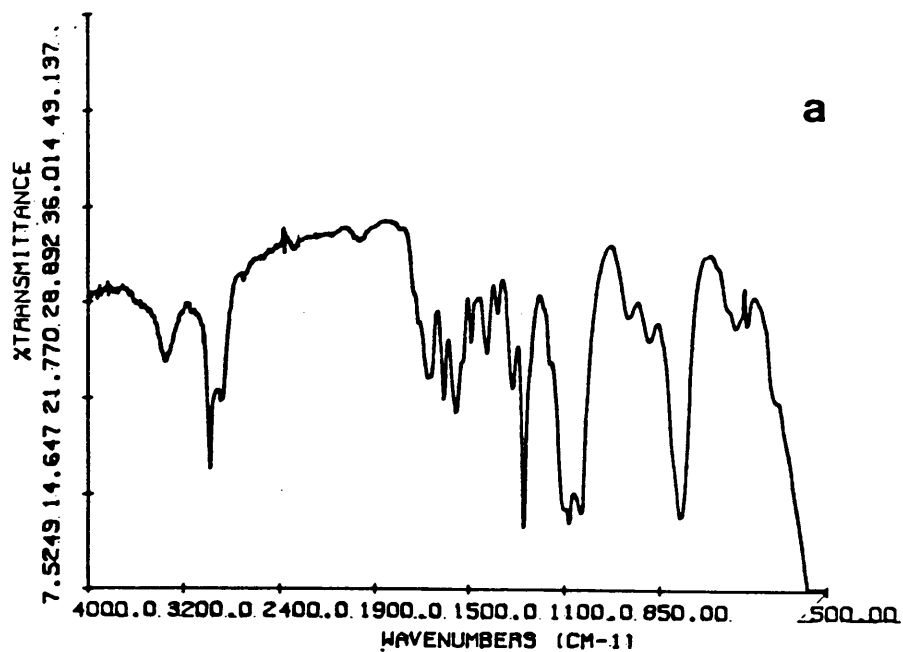
Figure 15. FTIR spectra of PSX urea (a) and PPO urea (b) segmented
copolymers

Table 9. Polyurea and polyurethane urea segmented
copolymers

| SERIES | SAMPLE | [ n ]* |
|--------|--------|--------|
| I | PSX1150-MDI 18 | 0.78 |
| | PSX2200-MDI 10 | 1.20 |
| | PSX5000-MDI 5 | 0.85 |
| | pPSX2600-MDI 9 | 0.56 |
| | pPSX5000-MDI 5 | 0.63 |
| | pPSX11700-MDI 12 | 0.70 |
| II | JEF2000-H20 | 0.68 |
| | PPO2000-H20 | 0.78 |
| | PPO2800-H20 | 1.05 |
| III | UR-PSX1150-8 | 0.61 |
| | UR-pPSX2600-8 | 0.55 |
| | UR-pPSX2600-16 | 0.52 |
| | UR-pPSX2600-24 | 0.52 |
| | UR-pPSX5300-8 | 0.63 |
| | UR-pPSX5300-16 | 0.55 |
| | UR-pPSX5300-24 | 0.55 |
| IV | PTMO2000-H20 | 1.09 |
| | UT-PSX1150-8 | 1.06 |
| | UT-PSX1150-16 | 0.61 |
| | UT-PSX1150-24 | 0.76 |
| | UT-PSX2200-8 | 0.78 |
| | UT-PSX2200-16 | 0.70 |
| | UT-PSX2200-24 | 0.61 |

* SERIES 1 in THF and OTHERS in DMAc at 25 ºC

where "UT" is the control polyurethane urea, PTMO2000-H20. For the latter two series of copolymers, the hard segment composition and content remained same as that of the control. The intrinsic viscosity values ranged from 0.5 to 1.0 dl/g, suggesting relatively high molecular weight was achieved.

The structural analysis, intrinsic viscosity data, and solubility of copolymers in polar solvents suggests that linear high molecular weight polyether ureas and polyether urethane ureas were successfully synthesized.


## 4 - 2. Thermal Analysis


The thermal transitions of polyurea and urethane-urea elastomers were detected by differential scanning calorimetry (DSC). The glass transition temperatures of polysiloxane and polypropylene oxide urea copolymers are shown in Table 10. Only the glass transition of the rubbery phase were observed. The endotherms at elevated temperatures corresponding to long range order or crystalline phase of hard segments and the Tg of the hard phase were not detected probably due to low levels of the urea content.

From Table 10, it can be noted that the soft segment Tg increases with increasing MDI content for both polydimethylsiloxane and poly(dimethyl-diphenyl)siloxane based polyureas. The increase can be attributed to larger amounts of urea linkages available for hydrogen bonding, which will restrict soft segment mobility. Also, poly(dimethyl-diphenyl)siloxane based polyureas exhibit higher Tg values for the soft phase compared to polydimethyl siloxane based polyureas indicating less phase separation. This higher degree of phase mixing results from increased polarity of the soft segment due to phenyl substituents on the siloxane backbone. This enhances the tendency for isolated urea sequences to be trapped in the rubbery matrix. Similarly, the polar aromatic end groups of PPO oligomer enhance phase mixing with the urea segments leading to higher Tg values compared to that of Jeffamine based polyurea at the same soft segment molecular weight and hard segment content. Higher

Table 10. Tg values for polyurea segmented copolymers

| SAMPLE | Tg ($^{\circ}$C)* | Tg SHIFT ($^{\circ}$C)** |
|--------|-------------------|--------------------------|
| PSX1150-MDI 18 | -115 | 4 |
| PSX2200-MDI 10 | -121 | 2 |
| PSX5000-MDI 5 | -122 | 1 |
| pPSX2600-MDI 9 | -58 | 25 |
| pPSX5300-MDI 5 | -66 | 12 |
| pPSX11700-MDI 2 | -80 | 4 |
| JEF2000-H20 | -56 | 19 |
| PPO2000-H20 | -46 | 24 |
| PPO2800-H20 | -58 | 12 |

* from the transition midpoint of DSC second scan
**relative to the oligomer itself

molecular weight difunctional PPO prepared via coordination polymerization using porphorin initiator results in better phase separated material as expected, and displays Tg values comparable to that of JEF2000-H20.

The DSC transitions of siloxane incorporated polyether ureas are shown in Table 11. An approximately 5 °C increase in the soft segment Tg was observed, compared to that of the control polyurea (JEF2000-H20). No trend was apparent for increasing siloxane content or molecular weight. The small increase in Tg indicated a high extent of phase mixing, possibly arising from the broadening molecular weight distribution of two types of soft segments. Also, the phenyl units of siloxane may have enhanced the polarity of the soft segment, thus solubilizing the urea segments as discussed earlier.

The DSC thermograms of siloxane incorporated polyurethane ureas are illustrated in Figure 16 and the transitions are summarized in Table 12. The glass transition temperatures of PTMO2000 oligomer occurs at -78 °C, followed by a melting endotherm at about 25 °C. From the soft segment glass transitions presented, it can be seen that the copolymers are highly phase separated materials with Tg shifts from Tg of the oligomer ranging from 0 to 7 °C. Increasing the amount of siloxane incorporation resulted in a decreasing Tg suggesting that higher degrees of phase separation were produced. This can be attributed to increasing urea linkages present in the copolymer as more amine terminated siloxane oligomers are introduced in the system. The greater polarity differences between hard and soft segments in ureas compared to urethanes lead to better phase separated materials. Moreover, the presence of the amorphous siloxane segments decreases the crystalline character of the soft PTMO segment, leading to more flexible chains and a lower Tg. As expected, the melting endotherm peak decreases with increasing siloxane content. A similar trend in thermal behavior is observed for both PSX1150 and PSX2200 incorporated polyurethane-ureas. At these low molecular weights, the phase separation of the copolymer is not affected by increasing molecular weight of the siloxane.

TGA experiments were conducted in order to study the thermal stability of polypropylene oxide ureas and polyurethane ureas. From Figure 17, it can be seen that the polyurea based

Table 11. DSC results of siloxane incorporated
polyether urea segmented copolymers

| SAMPLE | Tg* ( $^{o}$C ) |
|--------|-----------------|
| UR (CONTROL)** | -56 |
| UR-PSX1150-8 | -53 |
| UR-pPSX2600-8 | -51 |
| UR-pPSX2600-16 | -51 |
| UR-pPSX2600-24 | -50 |
| UR-pPSX5300-8 | -52 |
| UR-pPSX5300-16 | -51 |
| UR-pPSX5300-24 | -52 |

*   from the transition midpoint of the second
    scan
**JEF2000-H20

1. PTMO2000-H20
2. 8 Wt.% PSX1150
3. 16 Wt% PSX1150
4. 24 Wt% PSX1150
5. 8 Wt% PSX2200
6. 16 Wt% PSX2200
7. 24 Wt% PSX2200
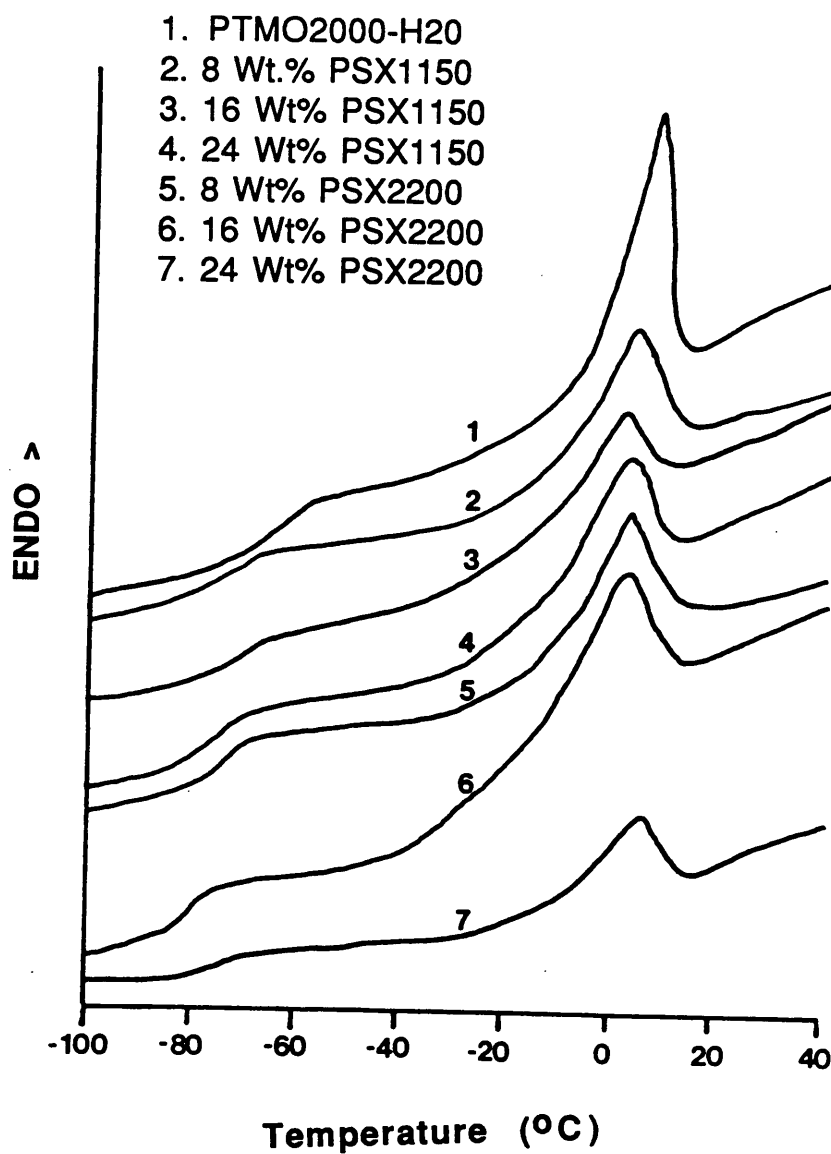
Figure 16. DSC thermograms of siloxane incorporated polyurethane-urea segmented copolymers

Table 12. DSC transitions of siloxane incorporated polyurethane urea segmented copolymers

| SAMPLE | Tg ($^{o}$C)* | Tm($^{o}$C) | Hf (J/g) |
|---|---|---|---|
| UT (CONTROL)** | -71 | 4 | 22.8 |
| UT-PSX1150-8 | -73 | 3 | 16.8 |
| UT-PSX1150-16 | -74 | 0 | 12.3 |
| UT-PSX1150-24 | -78 | 1 | 10.8 |
| UT-PSX2200-8 | -74 | 3 | 16.0 |
| UT-PSX2200-16 | -75 | 1 | 14.2 |
| UT-PSX2200-24 | -78 | 0 | 13.2 |

\* from the transition midpoint of the second scan
\*\*PTMO2000-H20

on PPO is about 30 to 40 °C more thermally stable than commercial Jeffamine based polyurea at the same soft segment molecular weight and hard segment content. Since the other components are identical, the improvement seems to arise from the end groups of polypropylene oxide oligomers. The aromatic amine terminated PPO appears to enhance the thermal stability of polyurea compared to aliphatic amine terminated commercial material as demonstrated earlier by Yoo (8).

Figure 18 illustrate the thermal degradation behavior of siloxane incorporated polyurethane urea copolymers. The results indicate that the initial degradation temperatures are increased by about 20 °C when 24 wt% of siloxane oligomers are incorporated into the system. The urea linkages are more thermally stable than urethane linkages due to stronger hydrogen bonding.


## 4 - 3. Stress-Strain Analysis


The engineering stress-strain curves for segmented polyether urea copolymers are shown in Figure 19-21. All curves are shown up to the ultimate strength of the sample, and the values of ultimate tensile strength and elongation at break are listed in Table 13. The stress-strain behavior of siloxane urea copolymers indicate that the mechanical response of these materials is strongly affected by soft segment length and the hard segment content as expected. Higher tensile strength is obtained as the hard segment content is increased since higher volume fraction of hard segments which results in more cohesive hard domains can serve as physical crosslinks and reinforcement fillers. The elongation at break is decreased with higher hard segment content as the soft segments become more constrained by the hard segment domains. The presence of phenyl units in the siloxane chain result in lower tensile properties at the same molecular weight perhaps due to higher phase mixing in the copolymer.

Figure 17. TGA spectra of polypropylene oxide urea segmented
copolymers
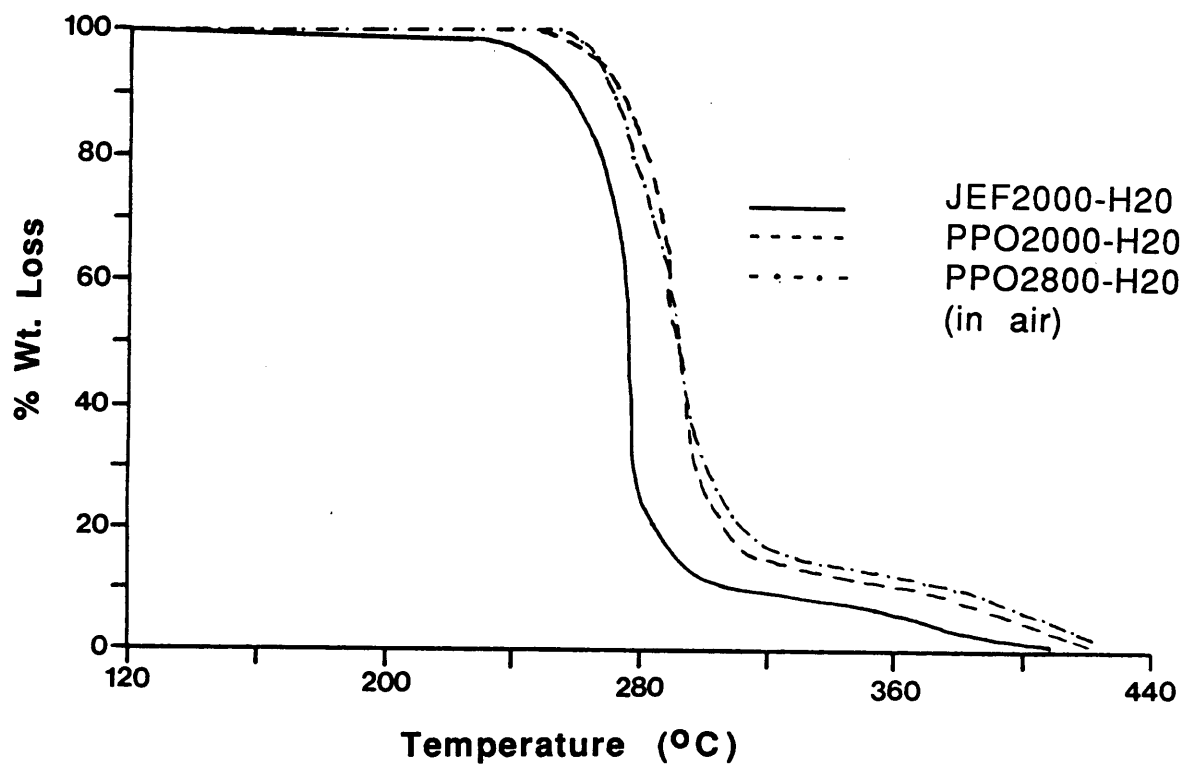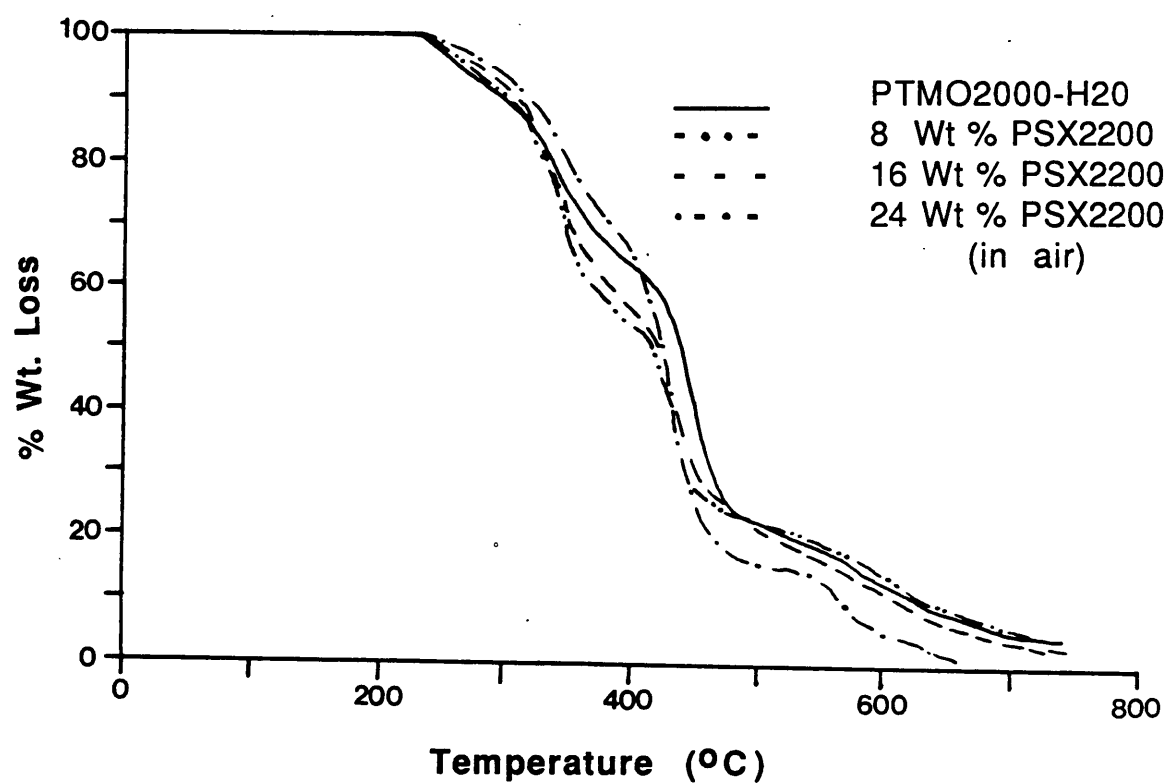
Figure 18. TGA spectra of siloxane incorporated polyurethane urea
segmented copolymers

For polypropylene oxide ureas, the tensile properties show marked improvement when the PPO oligomers synthesized by coordination polymerization are utilized instead of the commercial material (JEF). The low tensile strength exhibited by JEF2000-H20 can be attributed to the poor functionality of the oligomer which contain segments with less than two functional groups. This inhibit chain extension and lead to lower molecular weight materials as well as poorly defined structure, thus, reducing tensile strength. By utilizing highly difunctional PPO oligomers synthesized via living coordination polymerization, a well-defined high molecular weight segmented copolymers are prepared which show significant improvement in tensile properties; the tensile strength of PPO2800-H20 quadrupled that of JEF2000-H20 despite similar phase separation behavior of both materials. PPO2000-H20 display lower tensile strength than PPO2800-H20 due to higher phase mixing of the former as seen by DSC data.

The stress-strain behavior of the siloxane incorporated polyurea copolymers are illustrated in Figure 22 with results shown in Table 14. The curves display a steep initial slope, then bend over and continue with nearly constant slope to break. At low amount of siloxane incorporation (8 wt%), similar tensile properties as that of control polyurea (JEF2000-H20) are obtained, perhaps indicating a negligible effect on morphology. But with an increasing amount of siloxane incorporation, both tensile strength and elongation are decreased. This trend is observed for both pPSX2600 and pPSX5300 series. The reduction in tensile properties may be explained by the increasing soft segment size distribution introduced upon siloxane oligomer addition. Also, the increase in polarity of the soft segment due to phenyl units could enhance phase mixing of hard and soft segments. Both of these factors disturb the perfection of discrete hard segment domains with narrow size distribution which in turn lowers the tensile strength.

The effect of siloxane incorporation on the stress-strain behavior of PTMO based polyurethane urea is shown in Figure 23. The tensile strength and elongation data are reported in Table 15. The control polymer, without any siloxane incorporation, displayed a typical upturn in the stress-strain curve at large elongations attributed to the strain induced
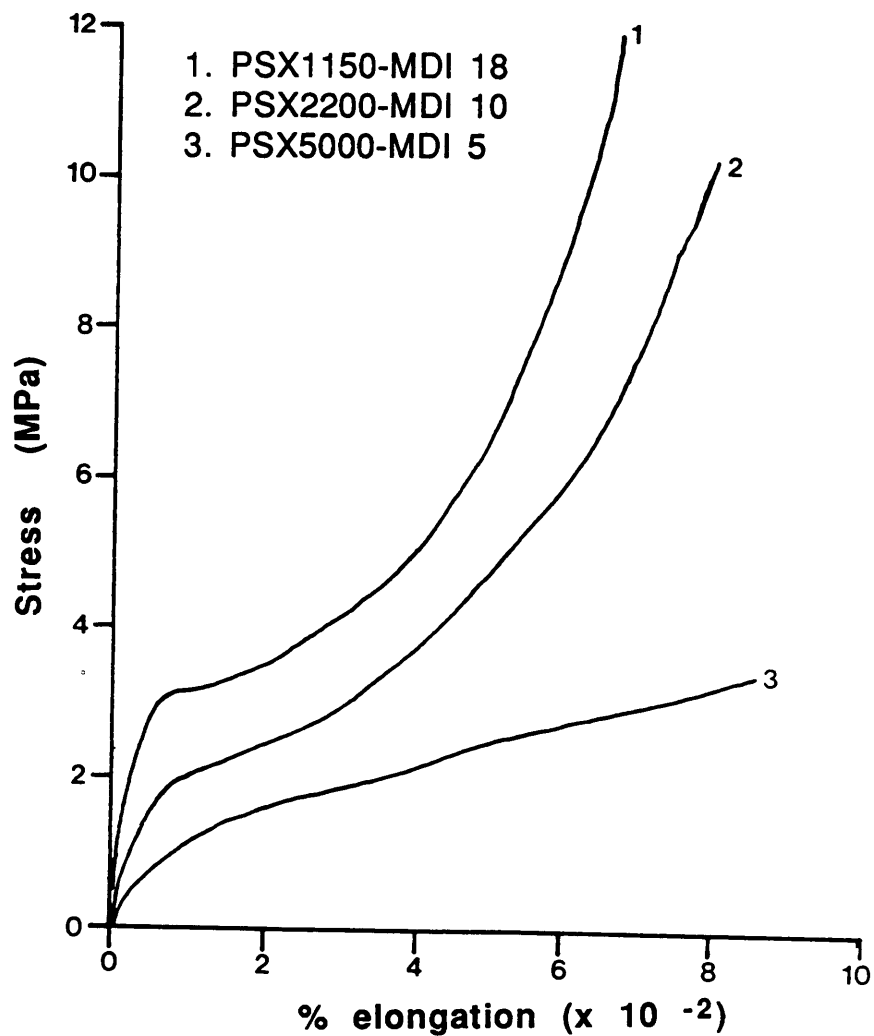
Figure 19. Stress vs % elongation for polydimethylsiloxane urea segmented copolymers (52)
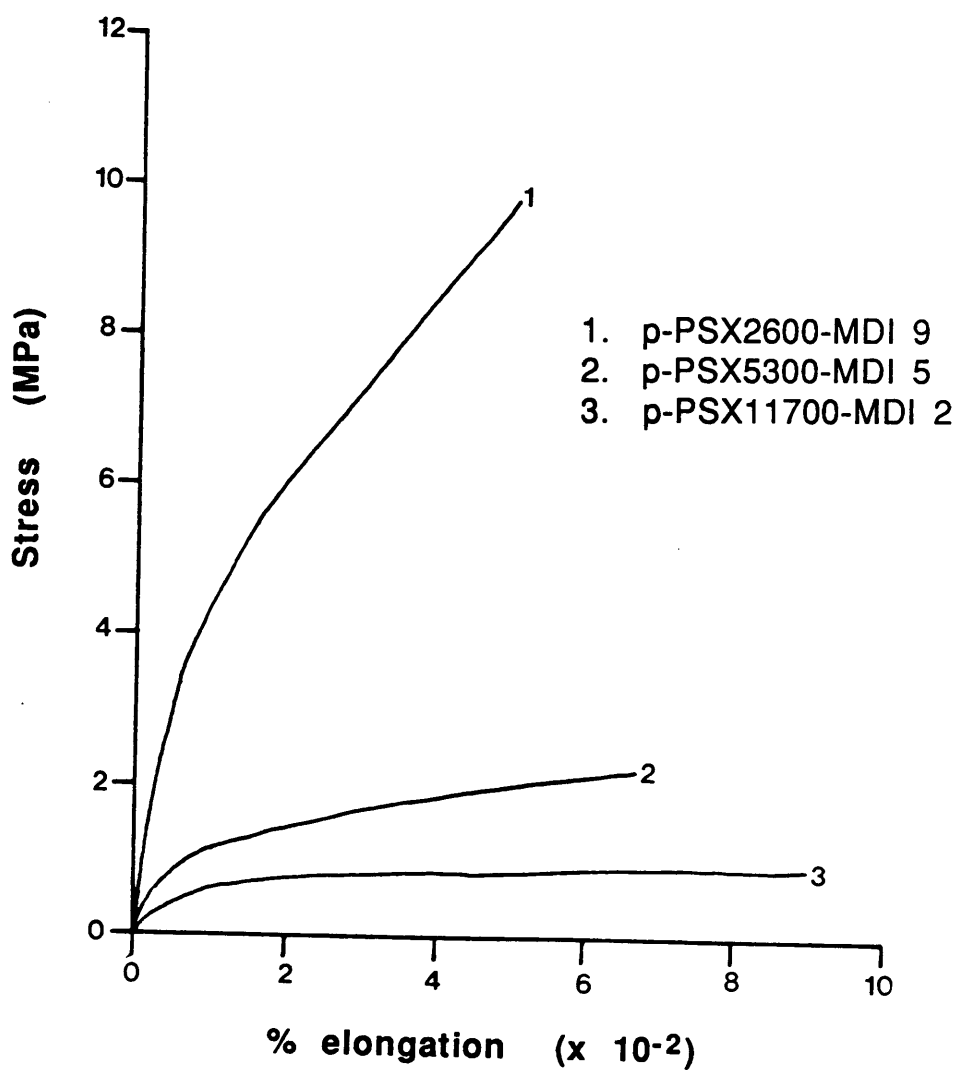
Figure 20. Stress vs % elongation of poly(dimethyl-diphenyl)siloxane-urea segmented copolymers (50 wt% diphenyl)
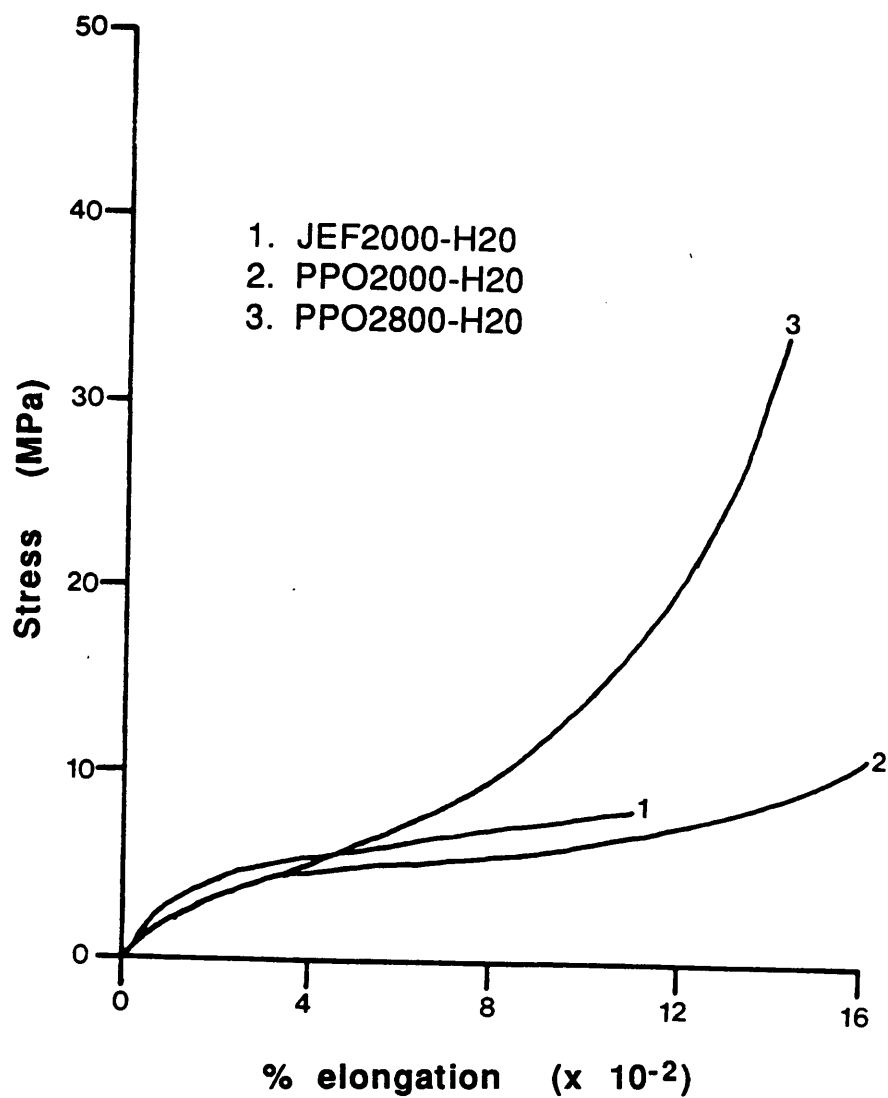
Figure 21. Stress vs % elongation for polypropylene oxide urea segmented copolymers

Table 13. Tensile strength of segmented polyurea
copolymers

| SAMPLE | TENSILE *<br>STRENGTH(MPa) | %ELONGATION |
|---|---|---|
| PSX1150-MDI 18 | 12.0 | 640 |
| PSX2200-MDI 10 | 10.2 | 750 |
| PSX5000-MDI 5 | 3.4 | 860 |
| pPSX2600-MDI 9 | 9.8 | 500 |
| pPSX5300-MDI 5 | 2.1 | 670 |
| pPSX11700-MDI 2 | 0.9 | 900 |
| JEF2000-H20 | 8.0 | 1075 |
| PPO2000-H20 | 11.0 | 1633 |
| PPO2800-H20 | 34.0 | 1400 |

*at break from an average of 5-10 samples

crystallization of the PTMO soft segments. By incorporating siloxane oligomers in the polymer, stress-induced crystallization is suppressed by the chemical irregularity of the soft segment, especially at 24 wt% addition. This leads to smaller upturn in the curve as well as lower tensile strength and higher extension. The decrease in PTMO crystallization has also been observed from DSC data where a smaller heat of fusion was detected. At the same amount of incorporation, similar stress-strain behavior is exhibited for both PSX1150 and PSX2200, showing little dependence of tensile strength on molecular weight. The amount of siloxane addition had a more significant effect on the stress and elongation at break. Approximately 10% decrease in the tensile strength and 10 to 25% increase in the elongation at break were observed for 8 and 16 wt% incorporation.

The hysteresis behavior of PTMO based polyurethane urea copolymers are also affected by siloxane incorporation as illustrated in Table 16. The stress softening behavior under cyclic loading conditions has been attributed to the plastic deformation of the hard segments. By adding siloxane soft segments, the percent hysteresis decreased from 77 to 52% approximately, at strain levels of 800%. This suggests that mechanical hysteresis increases with increasing stress-induced crystallization possibly due to the rearrangement of the stress-induced crystallites caused by deformation. Since stress-induced crystallization is suppressed by siloxane incorporation, it follows that the loss factor from the heat dissipation during cyclic deformation is decreased.

## 4 - 4. Characterization of Blends

Segmented polyurea and polyurethane copolymer blends are very complex due to their respective two-phase morphology. Miscibility can occur between hard segments of the blend constituents or between the soft phase or soft and hard phase through specific interactions such as hydrogen bonding, dipole-dipole interactions,and phenyl ring coupling. Segmented polyether urea copolymers derived from commercial PPO (JEF2000) soft segment and 20 wt%

Figure 22. Stress vs % elongation for siloxane incorporated
polyurea segmented copolymers

Table 14. Tensile stength of siloxane incoporated polyurea segmented copolymers

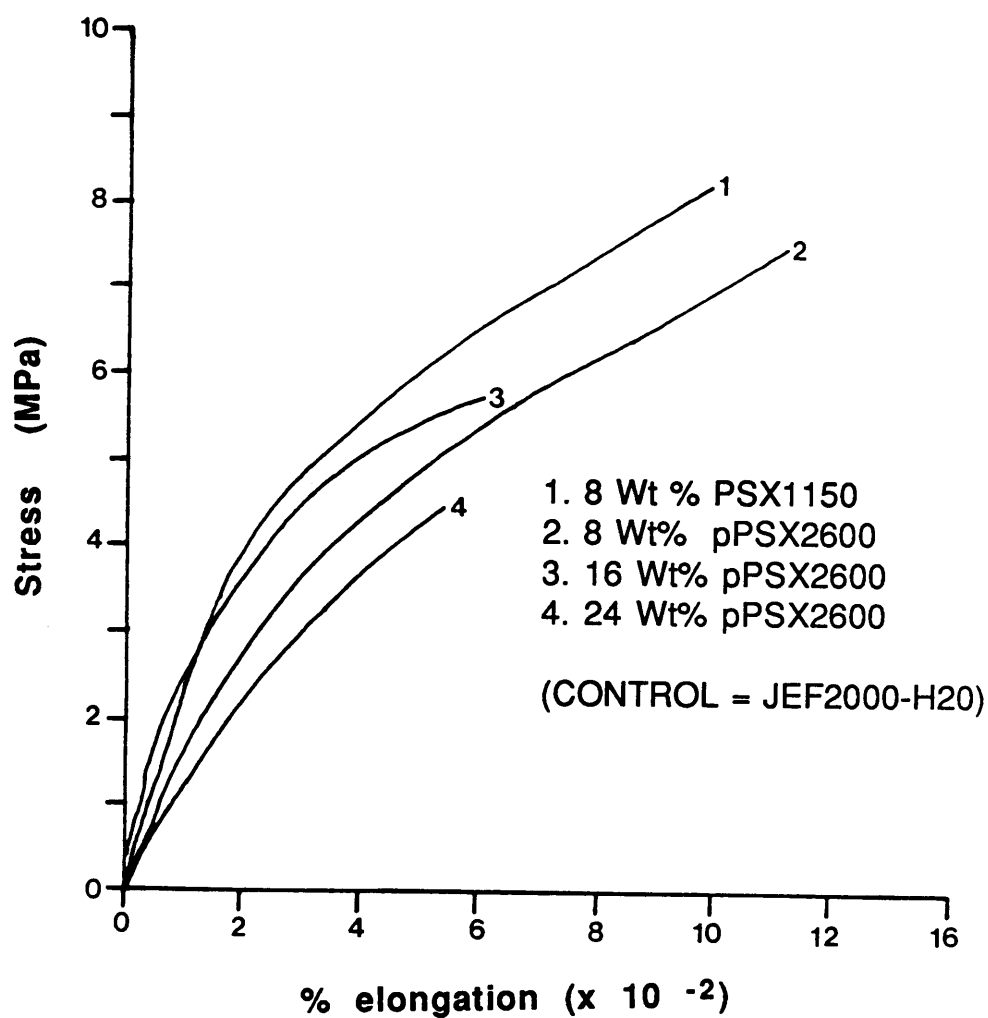| SAMPLE | TENSILE * STRENGTH (MPa) | %ELONGATION |
|---|---|---|
| UR (CONTROL)** | 8.0 | 1075 |
| UR-PSX1150-8 | 8.0 | 1000 |
| UR-pPSX2600-8 | 7.5 | 1100 |
| UR-pPSX2600-16 | 5.5 | 600 |
| UR-pPSX2600-24 | 4.5 | 500 |
| UR-pPSX5300-8 | 8.5 | 1350 |
| UR-pPSX5300-16 | 5.5 | 600 |
| UR-pPSX5300-24 | 5.0 | 500 |

* from an average of 5-10 samples
**JEF2000-H20
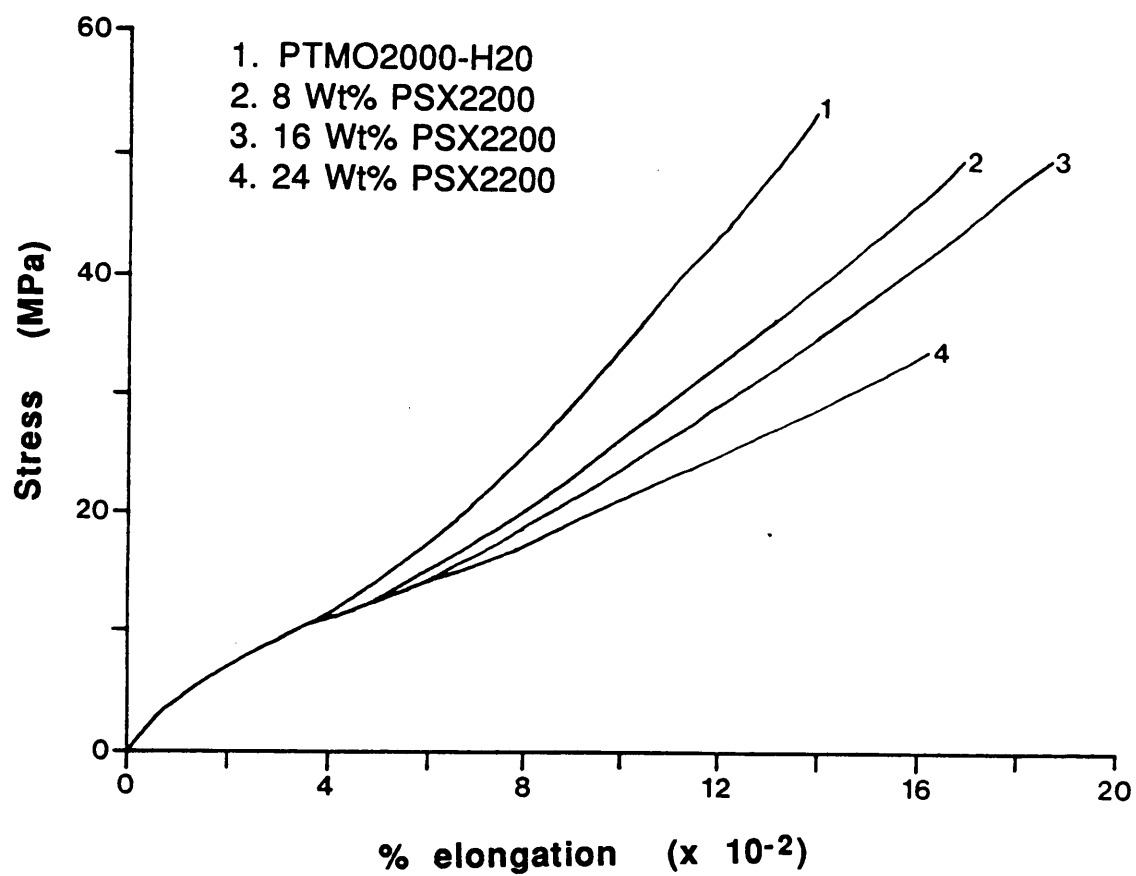
Figure 23. Stress vs % elongation for siloxane incorporated
polyurethane urea segmented copolymers

Table 15. Tensile strength of siloxane incorporated
polyurethane urea segmented copolymers

| SAMPLE | TENSILE * STRENGTH (MPa) | % ELONGATION |
|---|---|---|
| UT (CONTROL)** | 54.0 | 1362 |
| UT-PSX1150-8 | 48.0 | 1500 |
| UT-PSX1150-16 | 47.0 | 1796 |
| UT-PSX1150-24 | 33.0 | 1528 |
| UT-PSX2200-8 | 49.0 | 1684 |
| UT-PSX2200-16 | 49.0 | 1863 |
| UT-PSX2200-24 | 33.0 | 1582 |

* from an average of 5-10 samples
**PTMO-H20

MDI-ED hard segment content were blended with various siloxane urea copolymers. The blends were prepared by first dissolving each component in DMAC solvent at 10 wt/vol %. The solutions were then cast onto a clean glass plate and dried under conditions described in the experimental section. The preliminary evaluation of blend miscibility was based on observations of transparency of the solution mixture followed by the clarity and mechanical integrity of the films cast from solution.

The series of polydimethylsiloxane ureas blended with polyether urea resulted in mostly cloudy solutions, with films which exhibited macrophase separation and opacity (Table 17). Only the sample containing 5 wt% of PSX1150-MDI18 blended showed a clear solution and film which had mechanical integrity. This suggests that miscibility is enhanced by low siloxane contents and by high hard segment content via hydrogen bonding between hard segments of the blend constituents. In the case of poly(dimethyl-diphenyl) siloxane ureas, 5 wt% of pPSX2600-MDI9, pPSX5300-MDI5, and pPSX11700-MDI2 blended with polyether urea produced clear solutions and films. Unlike the polydimethylsiloxane urea series, miscibility occured even at very low urea content, which indicates that miscibility was not a result of hard segment interactions in these systems. Instead, interaction between the siloxane soft segment and urea hard segment of polyether urea may have been enhanced by the dipheny units on siloxane oligomer, which increased the polar nature of the soft segment to a certain extent. The 10 wt% of siloxane urea samples which were blended with polyether urea, all resulted in opaque films which exhibited gross macrophase separation. Further discussion of blend miscibility and properties which follow pertain only to those systems considered miscible by visual criteria mentioned here.

Figure 24 shows the DSC thermograms of blend systems that were considered compatible as judged by the optical clarity of the solvent cast films. Due to the low hard segment content, only the soft segment glass transitions were observed. The presence of a single Tg corresponding to the control material JEF2000-H20 seems to indicate homogeneous systems. However, this is probably due to rather small amounts of (5 wt%) siloxane urea copolymers present which makes it difficult to be detected by this technique. The results were very in-

Table 16. % hysteresis of siloxane incorporated
         polyurethane urea segmented copolymers

| SAMPLE | % HYSTERESIS * |
|---|---|
| UT (CONTROL) ** | 77.4 |
| UT-PSX1150-8 | 61.7 |
| UT-PSX1150-16 | 60.2 |
| UT-PSX1150-24 | 55.3 |
| UT-PSX2200-8 | 70.0 |
| UT-PSX2200-16 | 68.3 |
| UT-PSX2200-24 | 52.9 |

* at 800 % strain level from an average of 5 samples
** PTMO2000-H20

Table 17. Polyurea copolymer blend characteristics

| SAMPLE | WT% | CONDITION*** SOLUTION** | FILM |
|--------|-----|----------------------|------|
| UR*/PSX1150-MDI 18 | 95/5 | T | C |
| UR/PSX2200-MDI 10 | 95/5 | C | C |
| UR/PSX5000-MDI 5 | 95/5 | C | C |
| | | | |
| UR/pPSX2600-MDI 9 | 95/5 | T | T |
| UR/pPSX5300-MDI 5 | 95/5 | T | T |
| UR/pPSX11700-MDI 2 | 95/5 | T | T |
| | | | |
| UR/PSX1150-MDI 18 | 90/10 | C | C |
| UR/PSX2200-MDI 10 | 90/10 | C | C |
| UR/PSX5000-MDI 5 | 90/10 | C | C |
| | | | |
| UR/pPSX2600-MDI 9 | 90/10 | T | C |
| UR/pPSX5300-MDI 5 | 90/10 | C | C |
| UR/pPSX11700-MDI 2 | 90/10 | C | C |

\* UR= JEF2000-H20
\*\* in DMAc
\*\*\* T : transparent,  C : cloudy

1. JEF2000-H20
2. 5 Wt% PSX1150-MDI 18
3. 5  Wt% pPSX2600-MDI 9
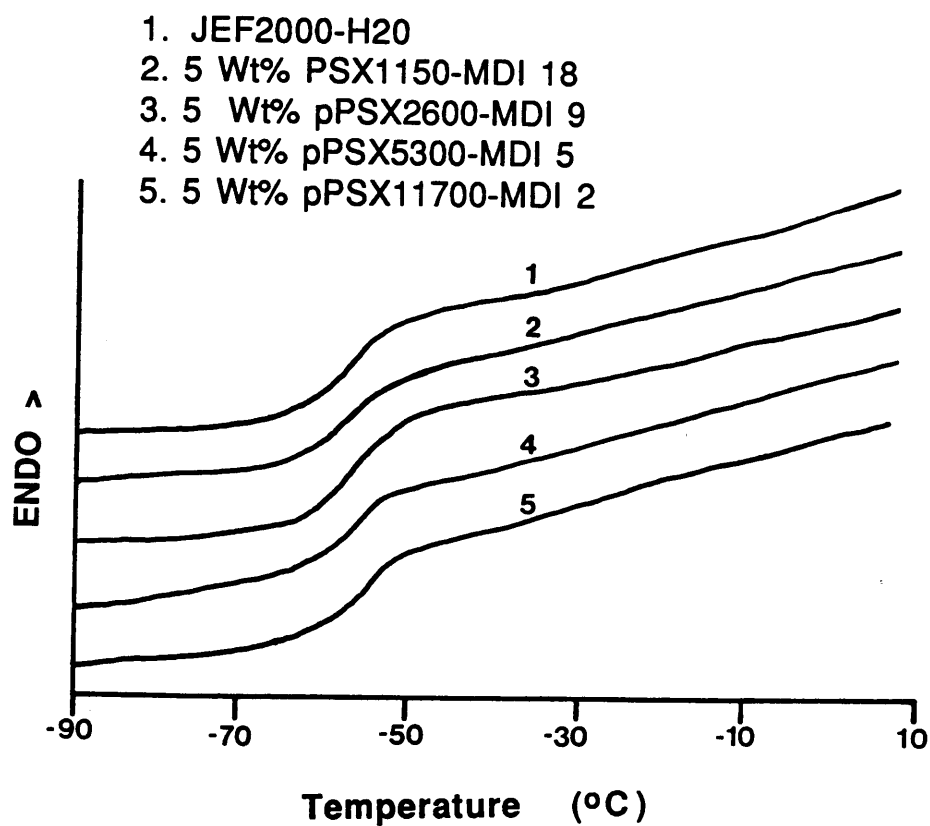4. 5 Wt% pPSX5300-MDI 5
5. 5 Wt% pPSX11700-MDI 2

Figure 24. DSC thermograms of polyurea copolymer blends

conclusive toward determining miscibility of the blends. Therefore, the transitions associated with the soft and hard segments were also measured by TMA.

Figure 25 and 26 illustrate the thermomechanical spectrum in penetration mode for the blend constituents and blend systems respectively. Two softening temperatures were observed corresponding to the soft segment glass transtion, followed by the onset of the flow region as the hard segment domains are disrupted. The soft segment Tg for polyurea copolymers determined by TMA are fairly consistent with DSC data. The broadness of the rubbery plateau decreased as the reinforcing hard segment content decreased. Since the reduction of hard segments mean less interchain hydrogen bonding (therefore less physical crosslinking points) the rubbery region is shortened and hard segment softening temperature is lowered. TMA thermograms of the blends consistently revealed the soft segment Tg around -50 °C and softening of the hard segment domain at temperatures above 180 ° C. These values correlated well with that of the control copolymer. Other softening points corresponding to the siloxane urea copolymers were not detected.

The stress-strain curves (Figure 27) for copolymer blends exhibit similar behavior as that of the control polyether urea (JEF2000-H20). The tensile strength and elongation at break are not affected noticeably by addition of small amount of siloxane urea copolymers. Since tensile properties of polyether urea are not detracted from blending small amounts of siloxane ureas, the blends are considered mechanically compatible. This supports the results obtained from thermomechanical analysis.

## 4 - 5. Surface Analysis

The surface composition of siloxane modified polyurea and polyurethane urea segmented copolymers was studied from X-ray photoelectron spectroscopy (XPS). The carbon 1s core-level spectra of siloxane incorporated polyureas are shown in Figure 28. In the spectrum, the main peak was assigned the value of 285.0 eV for the binding energy of carbon
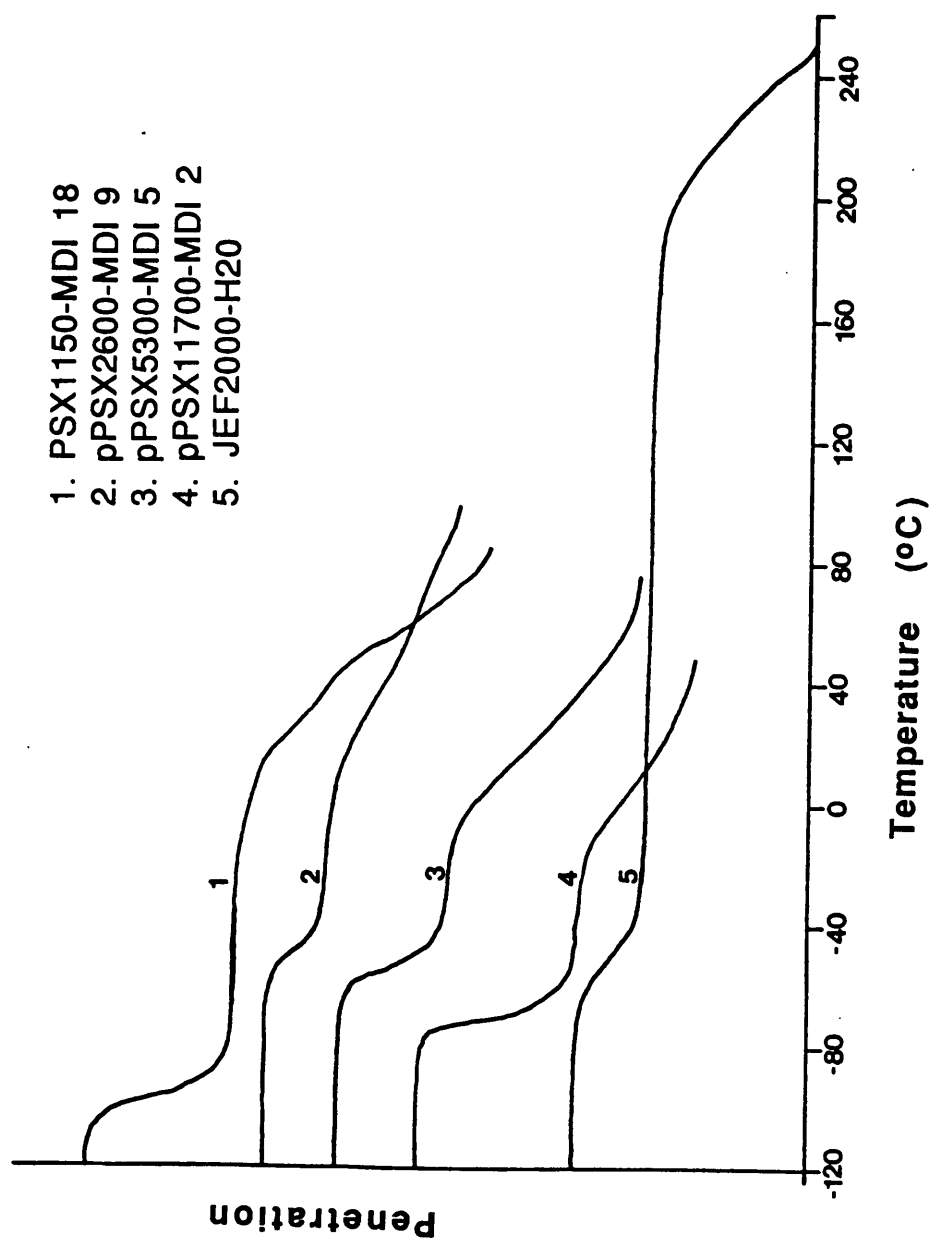
Figure 25. TMA spectra of polyurea segmented copolymers

1. PSX1150-MDI 18
2. pPSX2600-MDI 9
3. pPSX5300-MDI 5
4. pPSX11700-MDI 2
5. JEF2000-H20

Penetration

Temperature (°C)

1. UR/ PSX1150-MDI 18 (5 Wt%)
2. UR/pPSX2600-MDI 9  (5 Wt%)
3. UR/pPSX5300-MDI 5 (5 Wt%)
4. UR/pPSX11700-MDI 2 (5 Wt%)
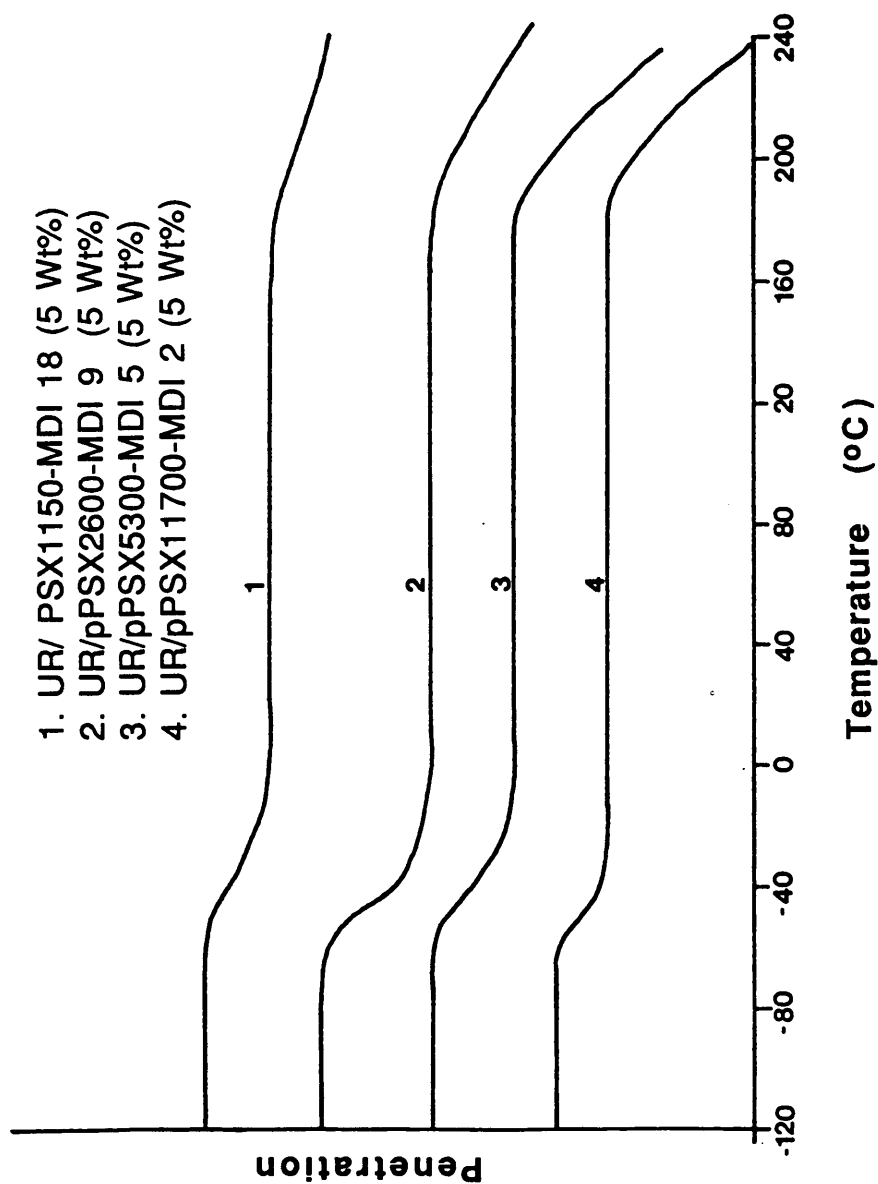
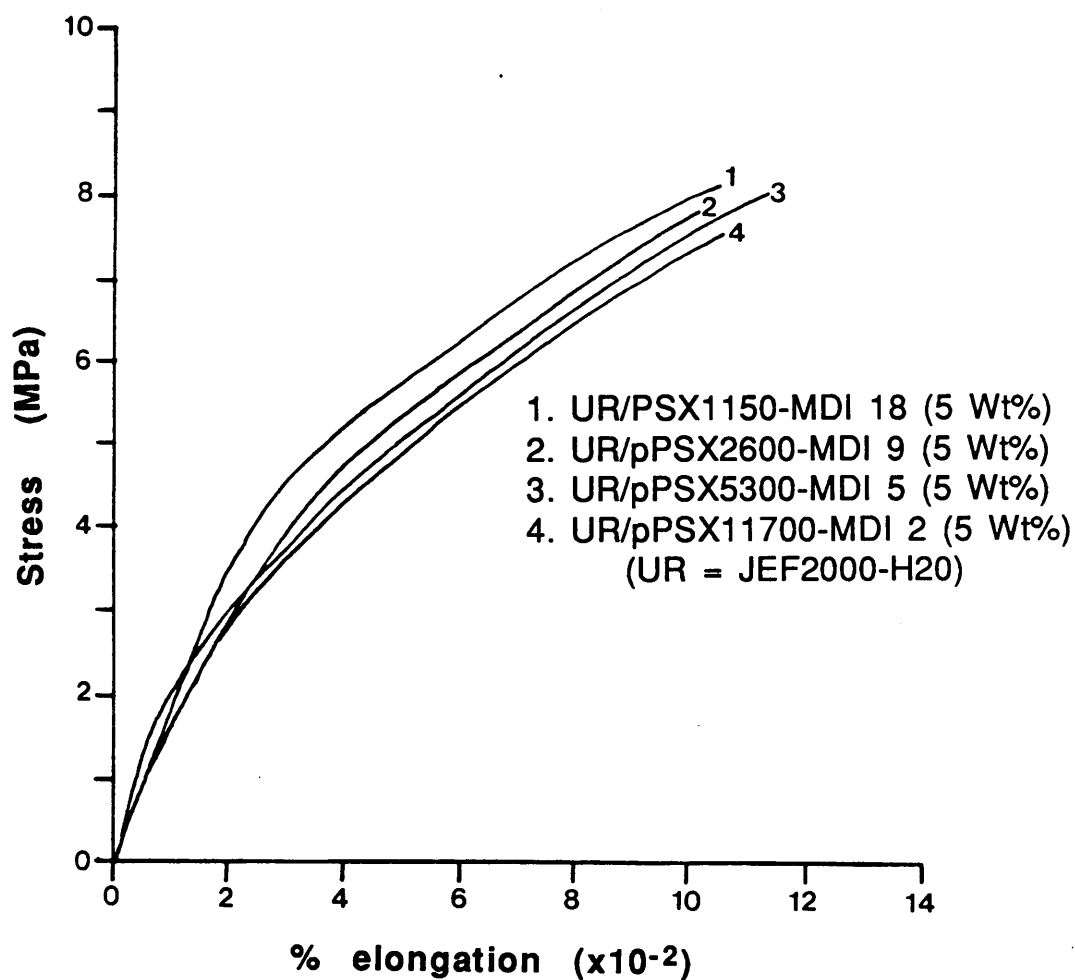Figure 26. TMA spectra of polyurea copolymer blends

Figure 27. Stress vs % elongation for polyurea copolymer blends

1s core level photoemission of the unsubstituted hydrocarbon. The strong higher binding energy subpeak, shifted 1.7 eV from the main peak, corresponds primarily to the carbon 1s core level photoemission of carbon singly bonded to oxygen, originating from the polypropylene oxide soft segment. It is apparent from the spectra that the intensity of this subpeak is decreasing with an increasing amount of siloxane incorporation. This is indicative of an increasing amount of siloxane on the surface at the expense of the PPO soft segment. Typical core level spectra of $O_{1s}$, $Si_{2p}$ and $N_{1s}$ for polyureas are shown in Figure 29. Unlike the carbon peak, these spectrum display narrow symmetrical singlets consistently for all samples. Table 18 gives the atomic ratios of silicon to oxygen calculated from the peak areas at the take-off angle of 90 ° (sampling depth of about 50 angstroms) and 10 ° (sampling depth of around 10 angstroms).

If complete domination of the surface by siloxane occurs the Si/O ratio should approach the value of 1.0, since each silicon is bonded to an oxygen according to chemical structure. The results show that Si/O ratios are much higher at the surface compared to those in the bulk indicating surface enrichment of siloxane soft segment. But the ratio does not attain the value of one even at bulk concentrations as high as 24 wt% siloxane suggesting a fairly large degree of phase mixing within the bulk. Also, the increase in Si/O ratio is relatively small with both the siloxane content and segment length. A similar trend is observed in comparing the the two angles indicating that a relatively small gradient of siloxane concentrations exists within the analysis depth. Based on these results, it can be postulated that the surface structure of siloxane incorporated polyether ureas is composed of a thick siloxane-rich overlayer intermixed with polypropylene oxide segments. Complete siloxane monolayer coverage is not observed due to the restricted mobility of the siloxane segments which are anchored at both ends by the urea hard segments within the bulk. As the siloxane segments phase segregate to the polymer-air surface, the polypropylene oxide segments which are covalently bonded to the same chain are also dragged to the surface to some extent. When the siloxane molecular weight increases, the longer segment attains more freedom of motion for segregation to the surface. In addition, the degree of phase mixing within the bulk plays an im-

portant role in determining surface segregation. This can be evidenced by comparing the Si/O ratios at 8 wt% siloxane incorporation. The highest value is obtained for the polydimethylsiloxane (PSX1150) despite longer segment length of poly(dimethyl-diphenyl)siloxane (pPSX2600, pPSX5300) series. This is a result of greater degree of phase mixing in the latter materials.

Similar surface behavior is also observed for the polyurea copolymer blends as shown in the carbon 1s spectra (Figure 30) and the Si/O ratios (Table 19). The carbon 1s peak is split into a doublet with contributions from C-C and C-O bonds. The intensity of C-O peak at 286.7 eV due to polypropylene oxide soft segment decreases with the addition of siloxane urea copolymers as the siloxane segment segregates to the surface. The decrease in intensity is highest for polydimethylsiloxane based polyurea, followed by the decreasing molecular weight of poly(dimethyl-diphenyl)siloxane series. This data corresponds well with the trends in the Si/O ratios which increase in relatively small amounts with regards to surface sensitive angle and increasing molecular weight of pPSX segments. The surface is enriched by siloxane to some extent but not to 100% which may be due to the restricted chain mobility caused by anchoring of both ends of the chain to urea segments. In addition, the presence of phenyl units enhance phase mixing with the polar hard segments within the bulk, suppressing phase segregation of the siloxane units to the surface. This is evidenced by the limiting Si/O ratio obtained from PSX1150-MDI18 blended with polyurea.

The carbon 1s spectra of siloxane incorporated polyurethane urea copolymers are shown in Figure 31 with Si/O ratios given in Table 20. The pronounced shoulder observed at 286.6 eV results from C-O bonds of PTMO soft segment. With increasing amount of siloxane incorporation, this peak disappears until a narrow symmetrical single peak is obtained. The Si/O ratios correlate well with this trend reaching the value of 1.0 at 16 to 24 wt% incorpo-ration of PSX2200, indicating complete surface enrichment by the siloxane segment. At lower molecular weight siloxane, the complete siloxane domination of the surface does not occur due to a decrease in mobility of the shorter chain. For large amount of siloxane incorporation, a surface concentration gradient exists indicating that the subsurfaces consist of a siloxane-
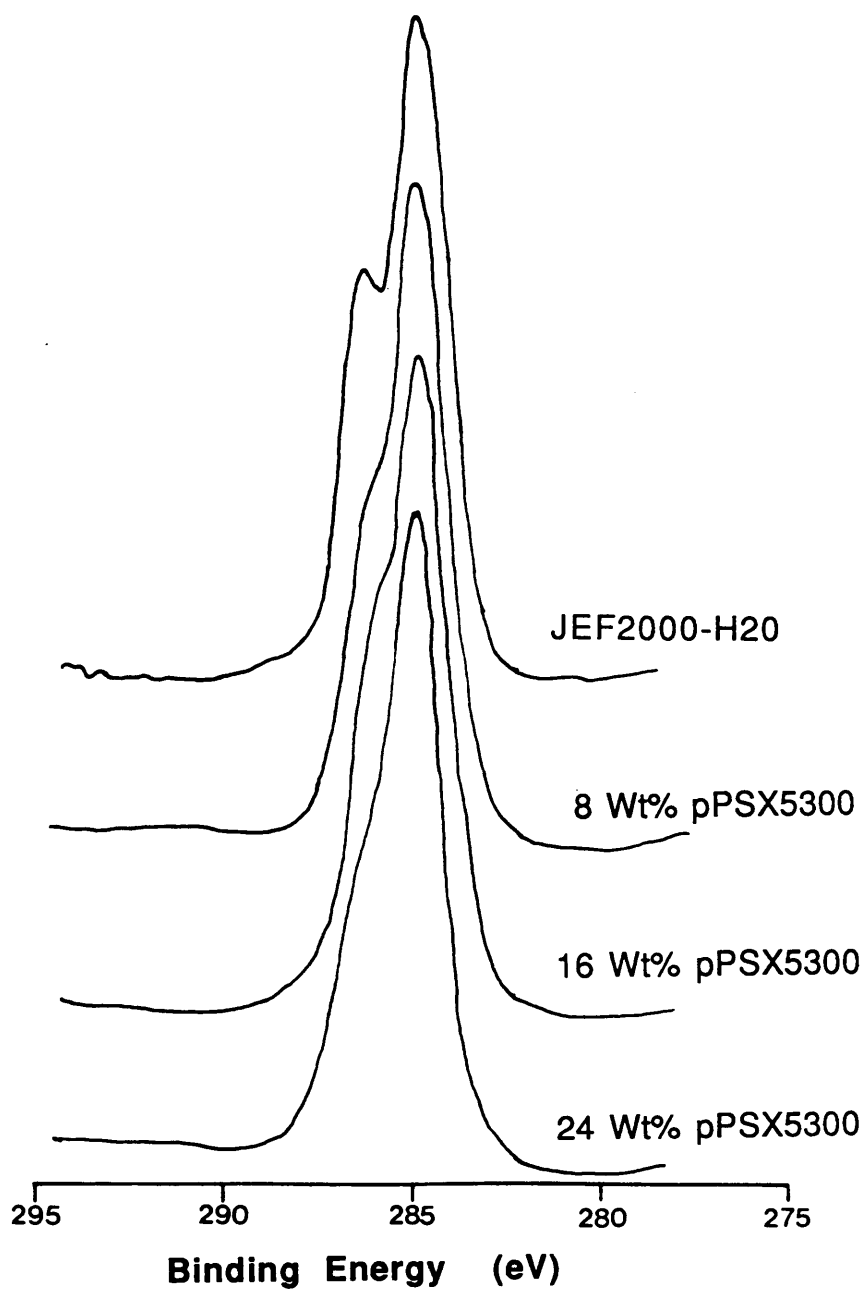
Figure 28. XPS carbon 1s spectra of siloxane incorporated polyurea segmented copolymers (90°)
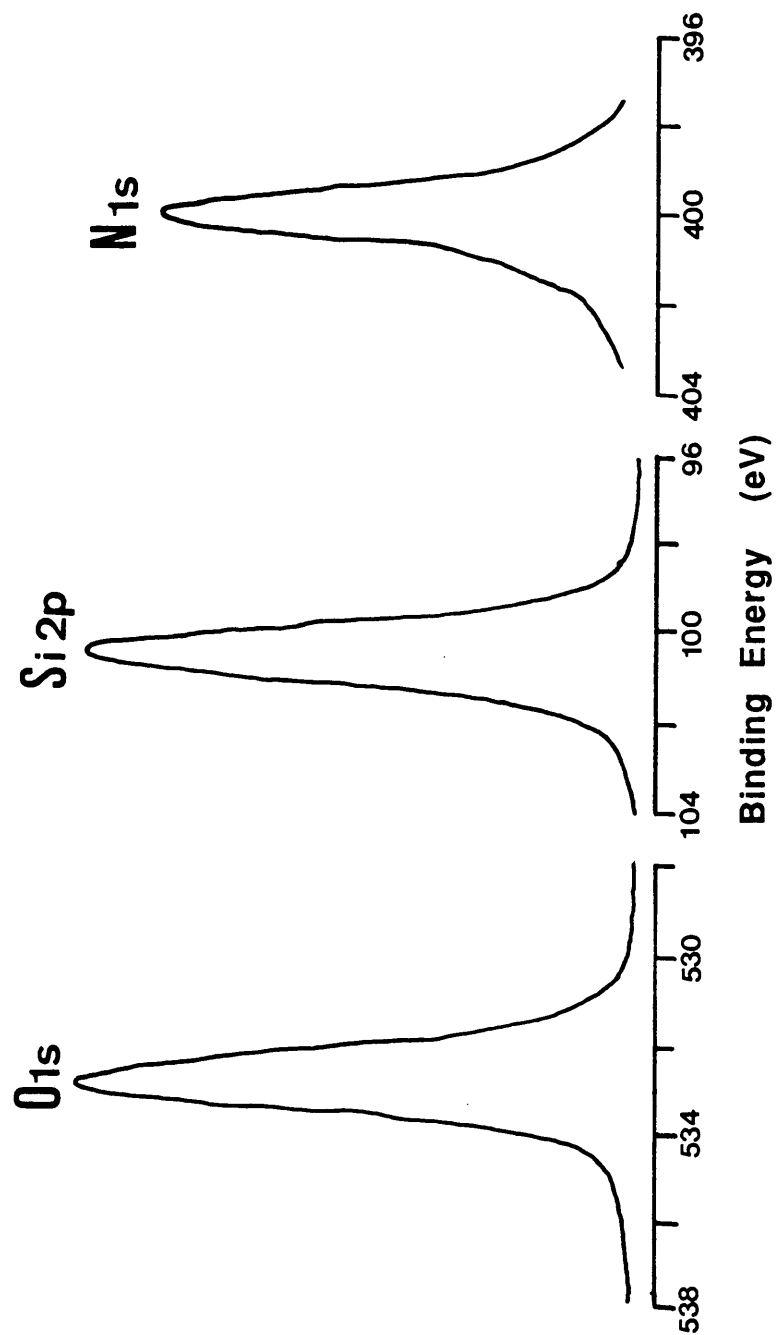
Figure 29. A typical XPS spectra of siloxane incorporated polyurea segmented copolymers (90°)

Table 18. The Si/O atomic ratios from XPS spectra of siloxane incorporated polyurea copolymers

| SAMPLE | Si/O RATIO | | |
| --- | --- | --- | --- |
| | BULK* | 90° | 10° |
| UR-PSX1150-8 | 0.05 | 0.57 | 0.75 |
| UR-pPSX2600-8 | 0.04 | 0.43 | 0.45 |
| UR-pPSX2600-16 | 0.09 | 0.50 | 0.60 |
| UR-pPSX2600-24 | 0.14 | 0.62 | 0.75 |
| UR-pPSX5300-8 | 0.05 | 0.51 | 0.62 |
| UR-pPSX5300-16 | 0.09 | 0.60 | 0.76 |
| UR-pPSX5300-24 | 0.15 | 0.72 | 0.85 |

* from calculations based on amount of components added

-UR : JEF2000-H20

rich layer of decreasing siloxane content with depth. These results indicate that polydimethylsiloxanes are more surface active compared to poly(dimethyl-diphenyl)siloxane segments due to greater incompatibility with the bulk polymer. Higher siloxane content is required for complete siloxane monolayer coverage, as a result of restricted segmental motion arising from phase mixing and anchoring of segment ends by hard segment domains.
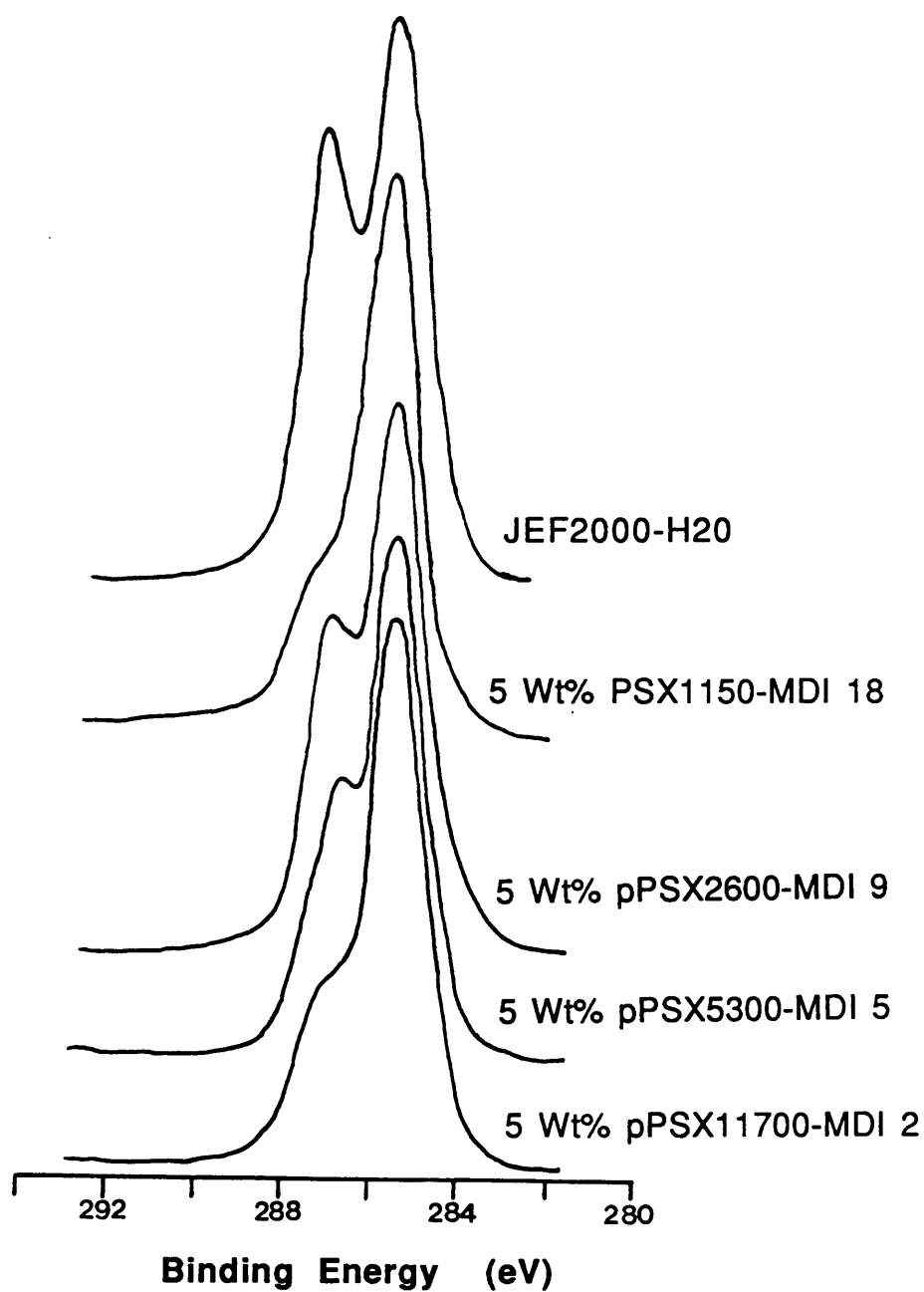
Figure 30. XPS carbon 1s spectra of polyurea copolymer blends (90°)

Table 19. The Si/O atomic ratios from XPS spectra of polyurea copolymer blends

| SAMPLE* | SI/O RATIO | | |
|---|---|---|---|
| | BULK** | 90° | 10° |
| UR/PSX1150-MDI 18 | 0.01 | 0.72 | 0.83 |
| UR/pPSX2600-MDI 9 | 0.02 | 0.50 | 0.60 |
| UR/pPSX5300-MDI 5 | 0.05 | 0.55 | 0.70 |
| UR/pPSX11700-MDI 2 | 0.10 | 0.62 | 0.75 |

\* 5 wt% of siloxane ureas blended with JEF2000-H20
\*\* from calculations based on amount of components added
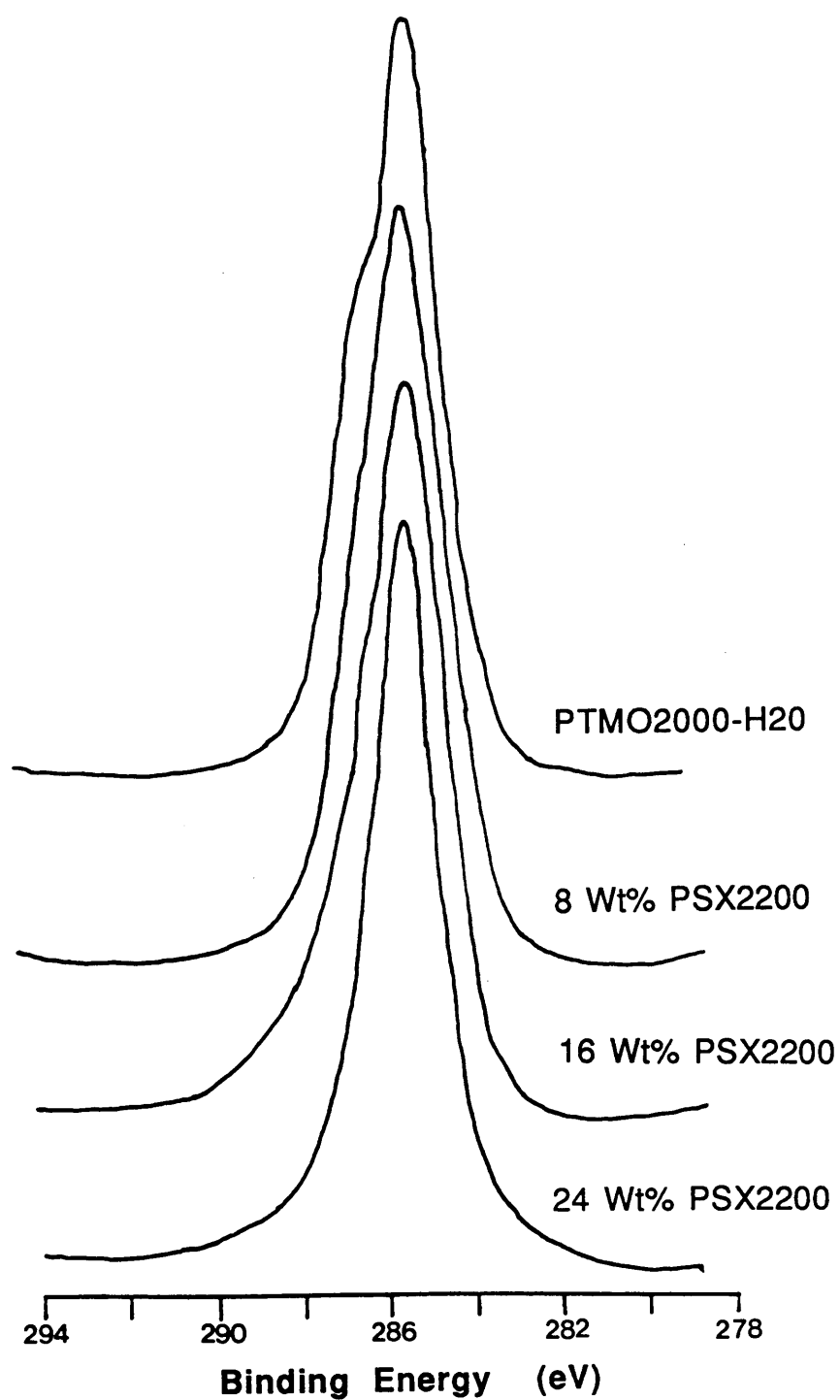
Figure 31. XPS carbon 1s spectra of siloxane incorporated polyurethane urea copolymers (90°)

Table 20. The Si/O atomic ratios from XPS spectra of
siloxane incorporated polyurethane urea
segmented copolymers

| SAMPLE | SI/O RATIO | | |
| --- | --- | --- | --- |
| | BULK* | 90° | 10° |
| UT**-PSX1150-8 | 0.06 | 0.70 | 0.77 |
| UT-PSX1150-16 | 0.13 | 0.75 | 0.80 |
| UT-PSX1150-24 | 0.20 | 0.81 | 0.97 |
| UT-PSX2200-8 | 0.07 | 0.70 | 0.76 |
| UT-PSX2200-16 | 0.14 | 0.74 | 1.00 |
| UT-PSX2200-24 | 0.22 | 0.84 | 1.00 |

* from calculations based on amount of components added
** PTMO2000-H20

# Chapter V. SUMMARY and CONCLUSIONS

The surface and bulk properties of siloxane modified segmented polyurea and polyurethane urea copolymers have been investigated. The modification was carried out in two ways: by blending various siloxane urea copolymers with control polyether urea; and by chemically incorporating various polysiloxane oligomers into the polymer backbone as a part of the soft segment in polyether urea and polyether urethane urea copolymers.

The solvent cast blends of siloxane urea and polypropylene oxide urea segmented copolymer resulted in clear films with inherent mechanical integrity only when the urea hard segment content was fairly high. This was attributed to an increased interaction between the hard segments of blend constituents. For poly(dimethyl-diphenyl)siloxane ureas, the presence of the polar phenyl units in the oligomer enhanced miscibility with polyether urea. Clear films were obtained for siloxane molecular weights ranging from 2600 - 11700 g/mol. In both cases, only small amounts of siloxane urea copolymers could be successfully blended.

The thermal analysis (DSC, TMA) of these blends exhibited a single soft segment Tg peak and a single hard segment softening temperature, indicating the two phase nature of the system. The thermal transitions of the blends corresponded to those of polypropylene oxide urea and were not affected by 5 wt% addition of siloxane urea copolymers. Similarly, the tensile strength and elongation at break of blends corresponded to those of polypropylene

oxide urea, indicating "mechanical compatibility" of the system. Although the bulk properties of polyether urea were not affected by blending small amounts of siloxane urea copolymers, the surface structure was changed. From XPS results, surface enrichment of siloxanes was observed for all blend systems. The level of siloxane concentration at the surface increased slightly with surface sensitive angle indicating that only a small concentration gradient exists within the sampling depth. Also, the presence of phenyl units on siloxane segment suppresses surface segregation to some extent due to enhanced phase mixing between soft and hard segments.

In siloxane incorporated polyether ureas, the incorporation of polydimethylsiloxanes were very limited due to the large solubility differences between siloxane and urea segments. Less difficulties were encountered for poly(dimethyl-diphenyl)siloxane incorporation due to higher polarity of the siloxanes. However, this led to a higher degree of phase mixing and affected both the thermal and mechanical properties of copolymer. The Tg of the soft segment increased slightly while the tensile strength and elongation at break decreased with increasing siloxane content. Similar trends in the surface compostion data as those observed from the blends are followed. The siloxane content and segment length did not affect the surface enrichment of siloxanes significantly. A relatively small gradient of siloxane content with analysis depth was observed.

For polydimethylsiloxane incorporated polyurethane ureas, the phase separation was enhanced while stress-induced crystallization was suppressed with increasing siloxane content. The decrease in tensile strength with siloxane content was offset by an increase in elongation at break and by smaller mechanical hysteresis loss. The surface enrichment of siloxanes occured at higher siloxane content and segment molecular weight.

In addition, the mechanical properties and thermal stability of segmented polyurea copolymers were much improved by utilizing well-defined polypropylene oxide oligomers, synthesized via living coordination polymerization, compared to polyureas prepared from commercial material (Jeffamines).

From the results obtained, it can be concluded that surface properties of segmented polyurea or polyurethane urea copolymers can be changed without detracting significantly from the bulk properties by physical or chemical blending of siloxanes in the system. In order to obtain siloxane enriched surface without loss of bulk properties, a careful balance must be maintained between several factors which include: the degree of phase mixing within the bulk; the siloxane content; and the siloxane segment length. The extent of phase mixing within the polymer bulk also affects the surface segregation behavior. Poly(dimethyl-diphenyl)siloxane ureas are more compatible with polyureas and urethanes, but show less surface segregation of siloxanes due to higher degree of phase mixing with urea components compared to polydimethylsiloxane ureas. Increasing the siloxane content or segment length results in higher surface concentration but changes the bulk properties noticeably and decreases the miscibility with polyurea/urethanes.

Therefore, to optimize conditions for surface enrichment of siloxanes in order to improve polyurea/urethane release capabilities, the suggested future studies include:

- A blend series of chain extended polydimethylsiloxane urea/urethane copolymers with polyurea/urethane segmented copolymers should be prepared and characterized.

- The effect of varying siloxane segment length and hard segment content on bulk and surface properties should further be examined.

- An investigation of the "release" properties of these systems might be of considerable academic and industrial interest.

*

# Bibliography

1.  A. J. G. Allen, *J. Colloid Sci.*, 14, 206, 1959.

2.  N. L. Jarvis, R. B. Fox, and W. A. Zisman, *Advan. Chem. Ser.*, No. 43, 317, 1964.

3.  N. M. Patel, D. W. Dwight, J. L. Hedrick, D. C. Webster, and J. E. McGrath, *Macromolecules*, 21, 2689, 1988.

4.  G. Reiss, *Encyclopedia of Polymer Eng. & Sci.*; K. I. Kroschwitz ed.; Wiley-Interscience: New York, Vol 2, 324, 1988.

5.  D. T. Clark and J. Peeling, *J. Polym. Sci., Polym. Chem. Ed.*, 14, 543, 1976.

6.  C. S. P. Sung and C. B. Hu, *J. Biomed. Mat. Res.*, 13, 45, 1979.

7.  D. W. Dwight, B. Beck, J. S. Riffle, and J. E. McGrath, *Polymer Prepr.*, 20(1), 702, 1979.

8.  Y. Yoo, *Ph.D. Dissertation*, VPI & SU, Blacksburg, VA, 1989

9.  I. Yilgor, J. S. Riffle and J. E. McGrath, *Reactive Difunctional Siloxane Oligomers, ACS Symposium Series*, 282, 161, 1985.

10. B. C. Arkles and W. R. Peterson, Jr., *Silicon Compounds, Resister and Review*, Petrarch Systerms, Levittown, Pa., 1979.

11. H. R. Allcock and F. W. Lampe, *Contemporary Polymer Chemistry*, Prentice-Hall, Inc., Englewood Cliffs, N. J., 1981.

12. M. G. Vonronskov, V. P. Mileshkevich and Y. A. Yuzheleskii, *The Siloxane Bond*, Plenium Press, N. Y., 1978. Feb. 22-26, 1982.

13. W. Noll, *Chemistry and Technology of Silicones*, Academic Press, N. Y., 1968.

14. H. K. Lichtenwalner and M. N. Sprung, *Encyclopedia of Polymer Science and Technology*, 12, 464, 1970.

15. B. B. Hardman and A. Torkelson, *Encyclopedia of Chemical Technology, 3rd ed.*, 20, 922, 1982.

16. J. E. McGrath, J. S. Riffle, A. K. Banthia, I. Yilgor and G. L. Wilkes, *Initiation of Polymerization, ACS Symposium Series*, 212, 145, 1983

17. P. M. Sormani, R. J. Minton and J. E. McGrath, *Ring-Opening Polymerization, ACS Symposium Series*, 286, 147, 1985.

18. S. W. Kantor, W. T. Grubb and R. C. Osthoff, *J. Amer. Chem. Soc.*, 76, 5190, 1954.

19. P. V. Wright and J. A. Semlyen, *Polymer*, 11, 462, 1969.

20. Z. Laita and M. Jelinek, *Polym. Sci. USSR*, 5, 342, 1964.

21. K. A. Andrianov and S. E. Iakushkima, *Polym. Sci. USSR*, 1, 221, 1960.

22. A. Noshay and J. E. McGrath, *Block Copolymers: Overview and Critical Survey*, Academic Press, N. Y., 1977.

23. J. C. Saam, D. J. Gordon and S. Lindsey, *Macromolecules*, 3(1), 1, 1970.

24. J. C. Saam and F. W. G. Fearon, *Ind. Eng. Chem., Prod. Res. Div.*, 10, 10, 1971.

25. M. Morton, A. A. Rembaum and E. E. Bostick, *J. Appl. Polym. Sci.*, 8, 2707, 1964.

26. G. Greber and A. Balciunas, *Macromol. Chem.*, 79, 149, 1964

27. G. Greber and A. Balciunas, *Farbe U. Lack*, 70, 249, 1964.

28. W. G. Davies and D. P. Jones, *Ind. Eng. Chem., Prod. Res. Div.*, 10(2), 168, 1971.

29. J. W. Dean, *J. Polym. Sci.*, B8, 10, 677, 1970.

30. G. L. Gaines and G. W. Bender, *Macromolecules*, 5, 82, 1972

31. A. K. Sha'ban, *M. S. Thesis*, VPI & SU, Blacksburg, VA, 1983.

32. A. Noshay, M. Matzner and T. C. Williams, *Ind. Eng. Chem., Prod. Res. Div.*, 12, 268, 1973.

33. A. Noshay, M. Matzner and C. N. Merrian, *J. Polym. Sci.*, A1, 9, 3147, 1971.

34. M. Matzner, A. Noshay and J. E. McGrath, *Trans. Soc. Rheol.*, 21-2, 273, 1977.

35. D. C. Webster, J. L. Hedrick and J. E. McGrath, *SAMPE Meeting Proceedings*, Reno, NV., April 3-5, 1984.

36. H. A. Vaughn, *J. Polym. Sci., Polym Lett. Ed.*, B7, 569, 1969.

37. J. S. Riffle, *Ph.D. Dissertation*, VPI & SU, Blacksburg, VA, 1980.

38. M. Varkis and A. V. Tobolsky, *J. Macromol. Sci., Phys.*, 4, 877, 1970.

39. D. G. LeGrand and G. L. Gaines, *Polym. Prepr., ACS Polym. Chem. Div.*, 11, 442, 1970.

40. I. Yilgor, G. L. Wilkes and J. E. McGrath, *Polym. Prepr., ACS Polym. Chem. Div.*, 23(1), 286, 1982.

41. I. Yilgor, J. S. Riffle, G. L. Wilkes and J. E. McGrath, *Polym. Bull.*, 8, 535, 1983.

42. B. C. Johnson, I. Yilgor and G. E. McGrath, *Polym. Prepr., ACS Polym. Chem. Div.*, 25(2), 54, 1984.

43. C. K. Riew, *Rubber Chem. Techn.*, 54(2), 374, 1981.

44. W. D. Bascom, R. L. Cottington and C. O. Timmons, *J. Appl. Polym. Sci., Appl. Polym. Symp.*, 32, 165, 1977.

45. C. Hepburn, *Polyurethane Elastomers*, Applied Science Publishers, London, 1982.

46. M. Pavlova, M. Draganova and P. Novakov, *Polymer*, 26, 1901, 1985.

47. G. N. Petrov and A. S. Lykin, *Polym. Sci. USSR*, 20, 1351, 1979.

48. N. S. Schneider and W. Matter, *Polym. Eng. Sci.*, 19, 1122, 1979.

49. M. Xu, W. J. MacKnight, C. H. Y. Chen and E. L. Thomas, *Polymer*, 25, 1807, 1984.

50. K. Oguro, N. Kunii, H. Nishimura and T. Doi, *Magic of Polyurethane*, SPI Inc., N. Y. 1985.

51. A. Lilaonitkul and S. L. Cooper, *Advances in Urethane Science and Technology*, 7, 163, 1979.

52. D. Tyagi, I. Yilgor, G. L. Wilkes and J. E. McGrath, *Polymer*, 25, 1807, 1984.

53. B. Bengston, C. Ferger and W. J. MacKnight, *Polymer*, 26, 895, 1985.

54. T. A. Speckhard, G. VerStrate, P. E. Gibson and S. L. Cooper, *Polym. Eng. Sci.*, 23, 337, 1983.

55. T. A. Speckhard and S. L. Cooper, *Rubber Chemistry and Technology*, 59, 3, 405, 1986.

56. T. A. Speckhard, P. E. Gibson, S. L. Cooper, V. S. C. Chang and J. P. Kennedy, *Polymer*, 26, 55, 1985.

57. J. A. Miller, S. B. Lin, K. K. S. Hwang, K. S. Wu, P. E. Gibson and S. L. Cooper, *Maromolecules*, 18, 32, 1985.

58. L. L. Harrell Jr., *Macromolecules*, 2, 6, 607, 1969.

59. C. S. Schollenberger, *Polyurethane Technology*, P. F. Bruins ed., Wiley-Interscience, N. Y. 1969.

60. M. A. Mendelsohn, F. W. Navish Jr. and D. Kim, *Rubber Chemistry and Technology*, 58, 5, 997, 1985.

61. M. V. Pandya, D. D. Deshpande and D. G. Hundiwal, *British Polymer Journal*, 19, 1, 1987.

62. J. A. Miller, S. B. Lin, K. S. Hwang, K. S. Wu, P. E. Gibson and S. L. Cooper, *Macromolecules*, 18, 32, 1985.

63. S. L. Cooper and A. V. Tobolsky, *J. Appl. Polym. Sci.*, 10, 1837, 1966.

64. R. Bonart, *J. Macromol. Sci. Phys.*, B2, 115, 1968.

65. S. B. Clough and N. S. Schneider, *J. Macromol. Sci. Phys.*, B2, 553, 1968.

66. L. M. Leung and J. T. Koberstein, *Macromolecules*, 19, 706, 1986.

67. R. Bonart and E. H. Muller, *J. Macromol. Sci., Phys.*, B10, 177, 1974.

68. Y. Camberlin and J. P. Pascault, *J. Polym. Sci., Polym. Chem. Ed.*, 21, 415, 1983.

69. C. S. P. Sung and N. S. Schneider, *Macromolecules*, 8, 68, 1975.

70. M. Xu, W. J. MacKnight, C. H. Y. Chen-Tsai and E. L. Thomas, *Polymer*, 28, 2183, 1987.

71. R. Bonart, L. Morbitzer and G. Hentze, *J. Macromol. Sci. Phys.*, B3, 337, 1969.

72. R. Bonart, L. Morbitzer and E. H. Muller, *J. Macromol. Sci. Phys.*, B9, 447, 1974.

73. J. Blackwell and K. H. Gardner, *Polymer*, 29, 13, 1979.

74. J. Blackwell, M. R. Nagarajan and T. B. Hoitnik, *Polymer*, 23, 950, 1982.

75. J. Blackwell and C. D. Lee, *J. Polym. Sci. Polym. Phys. Ed.*, 21, 2169, 1983.

76. J. W. C. Van Bogart, P. E. Gibson and S. L. Cooper, *J. Polym. Sci. Polym. Phys. Ed.*, 21, 65, 1983.

77. J. T. Koberstein and R. S. Stein, *J. Polym. Sci. Polym. Phys. Ed.*, 21, 1439, 1983.

78. J. A. Miller and S. L. Cooper, *J. Polym. Sci. Polym. Phys. Ed.*, 23, 1065, 1985.

79. J. A. Miller, G. Pruckmayr, E. Epperson and S. L. Cooper, *Polymer*, 26, 1915, 1985.

80. D. R. Paul and J. W. Barlow, *J. Macromol. Sci. Rev. Macromol. Chem.*, C18(1), 109, 1980.

81. D. R. Paul and S. Newman, *Polymer Blends*, Academic Press, N. Y. 1978.

82. P. J. Flory, *Principles of Polymer Chemistry*, Cornell Univ. Press, Ithaca, N. Y. 1962.

83. J. H. Hildebrand and R. L. Scott, *The Solubility of Non-electrolytes*, Reinhold, N. Y. 1950.

84. O. Olabisi, L. M. Robeson and M. T. Shaw, *Polymer-Polymer Miscibility*, Academic Press, N. Y. 1978.

85. A. J. Yu, *Copolymers, Polyblends and Composites, Adv. Chem. Ser.*, 142, 2, 1975.

86. T. K. Kwei, G. D. Patterson and T. Wang, *Macromolecules*, 9, 780, 1976.

87. E. Roerdink and G. Challa, *Polymer Journal*, 21, 5, 509, 1980.

88.  M. Iskander, C. Tran, L. M. Robeson and J. E. McGrath, *Polym. Eng. Sci.*, 23(12), 682, 1983.

89.  H. W. Bonk, A. A. Sardanopoli, H. Ulrich and A. A. R. Sayigh, *J. Elastopl.*, 3, 157, 1971.

90.  C. G. Seefried, J. V. Koleske and F. E. Critchfield, *Polym. Eng. Sci.*, 16(11). 771. 1976.

91.  J. Piglowski, T. Skowronski and B. Masiulanis, *Ang. Makromol. Chem.*, 85, 129, 1980.

92.  J. Piglowski and W. Lakawski, *Ang. Makromol. Chem.*, 84, 163, 1980.

93.  C. B. Wang and S. L. Cooper, *J. Appl. Polym. Sci.*, 26, 2989, 1981.

94.  D. T. Hourston and I. D. Hughes, *J. Appl. Polym. Sci.*, 26, 3467, 1981.

95.  P. K. Bandyapadhay and M. T. Shaw, *J. Appl. Poly. Sci.*, 27, 4323, 1982.

96.  F. Xiao, D. Shen, X. Zhang, S. Hu and M. Xu, *Polymer*, 28, 2335, 1987.

97.  P. Knaub, Y. Camberlin and J. F. Gerard, *Polymer*, 29, 1365, 1988.

The vita has been removed from
the scanned document